Low-Intensity Pulsed Ultrasound Enhances Angiogenesis and Ameliorates Left Ventricular Dysfunction in a Mouse Model of Acute Myocardial Infarction

Tomohiko Shindo, Kenta Ito, Tsuyoshi Ogata, Kazuaki Hatanaka, Ryo Kurosawa, Kumiko Eguchi, Yuta Kagaya, Kenichiro Hanawa, Kentaro Aizawa, Takashi Shiroto, Sachie Kasukabe, Satoshi Miyata, Hirofumi Taki, Hideyuki Hasegawa, Hiroshi Kanai, Hiroaki Shimokawa

Objective—Left ventricular (LV) remodeling after acute myocardial infarction still remains an important issue in cardiovascular medicine. We have recently demonstrated that low-intensity pulsed ultrasound (LIPUS) therapy improves myocardial ischemia in a pig model of chronic myocardial ischemia through enhanced myocardial angiogenesis. In the present study, we aimed to demonstrate whether LIPUS also ameliorates LV remodeling after acute myocardial infarction and if so, to elucidate the underlying molecular mechanisms involved in the beneficial effects of LIPUS.

Approach and Results—We examined the effects of LIPUS on LV remodeling in a mouse model of acute myocardial infarction, where the heart was treated with either LIPUS or no-LIPUS 3 times in the first week (days 1, 3, and 5). The LIPUS improved mortality and ameliorated post–myocardial infarction LV remodeling in mice. The LIPUS upregulated the expression of vascular endothelial growth factor, endothelial nitric oxide synthase, phosphorylated ERK, and phosphorylated Akt in the infarcted area early after acute myocardial infarction, leading to enhanced angiogenesis. Microarray analysis in cultured human endothelial cells showed that a total of 1050 genes, including those of the vascular endothelial growth factor signaling and focal adhesion pathways, were significantly altered by the LIPUS. Knockdown with small interfering RNA of either β1-integrin or caveolin-1, both of which are known to play key roles in mechanotransduction, suppressed the LIPUS-induced upregulation of vascular endothelial growth factor. Finally, in caveolin-1–deficient mice, the beneficial effects of LIPUS on mortality and post–myocardial infarction LV remodeling were absent.

Conclusions—These results indicate that the LIPUS therapy ameliorates post–myocardial infarction LV remodeling in mice in vivo, for which mechanotransduction and its downstream pathways may be involved. (***Arterioscler Thromb Vasc Biol*. 2016;36:1220-1229. DOI: 10.1161/ATVBAHA.115.306477.)**

Key Words: caveolae ■ caveolin-1 ■ integrins ■ myocardial infarction ■ myocardial ischemia

Downloaded from http://atvb.ahajournals.org/ by guest on February 21, 2017

Among the public health issues during the past 50 years, ischemic heart disease has been one of the world's top killer diseases.[1] Recent progress in emergency care and patient management has improved the prognosis of patients with acute myocardial infarction (AMI).[2,3] However, left ventricular (LV) remodeling after AMI still remains an unsolved problem in cardiovascular medicine. Thus, it is crucial to develop new therapeutic strategies to ameliorate post–myocardial infarction (MI) LV remodeling. We have previously demonstrated that low-energy extracorporeal cardiac shock wave therapy improves myocardial ischemia in a porcine model of chronic myocardial ischemia and patients with severe angina pectoris through enhanced myocardial angiogenesis.[4–7] Recently, we have further demonstrated that low-intensity pulsed ultrasound (LIPUS) therapy also induces angiogenesis and ameliorates myocardial ischemia in a porcine model of chronic myocardial ischemia.[8] LIPUS is also used for the treatment of patients with several diseases in orthopedics, dentistry, and brain stimulation.[9–13] However, it remains to be examined what molecular mechanisms are involved in the LIPUS-induced beneficial effects.

Vascular endothelial cells cover the inner surface of blood vessels and are directly subjected to blood flow–induced mechanical stimuli including shear stress. These stimuli invoke specific responses within the cells, leading to changes in their intrinsic structure and function.[14] Endothelial cells

Received on: August 26, 2015; final version accepted on: April 3, 2016.

From the Department of Cardiovascular Medicine, Graduate School of Medicine (T. Shindo, K.T., T.O., K. Hatanaka, R.K., K.E., Y.K., K. Hanawa, K.A., T. Shiroto, S.K., S.M., H.S.) and Department of Electronic Engineering, Graduate School of Engineering and Division of Biomedical Measurements and Diagnostics, Graduate School of Biomedical Engineering (H.T., H.H., H.K.), Tohoku University, Sendai, Japan.

This manuscript was sent to Qingbo Xu, Consulting Editor, for review by expert referees, editorial decision, and final disposition.

The online-only Data Supplement is available with this article at http://atvb.ahajournals.org/lookup/suppl/doi:10.1161/ATVBAHA.115.306477/-/DC1.

Correspondence to Kenta Ito, MD, PhD, Department of Cardiovascular Medicine, Tohoku University Graduate School of Medicine, 1-1 Seiryo-machi, Aoba-ku, Sendai 980-8574, Japan. E-mail ito-kenta@cardio.med.tohoku.ac.jp

© 2016 American Heart Association, Inc.

Nonstandard Abbreviations and Acronyms	
AMI	acute myocardial infarction
eNOS	endothelial nitric oxide synthase
ERK1/2	extracellular signal-regulated kinase 1/2
FAK	focal adhesion kinase
HUVEC	human umbilical vein endothelial cells
LIPUS	low-intensity pulsed ultrasound
MI	myocardial infarction
siRNA	small interfering RNA
VEGF	vascular endothelial growth factor

may sense these stimuli and convert them into a sequence of biological responses. Caveolae are flask-like invaginations of the plasma membrane with 40 to 80 nm in diameter and are organized by caveolins.[15,16] One of the aspects of caveolae is known to be flow-sensing organelles converting mechanical stimuli into chemical signals transmitted into the cells, so-called mechanotransduction.[15] Caveolins have been shown to bind to a variety of proteins involved in signaling pathways, such as G-protein subunits, tyrosine kinases, nitric oxide synthase, small guanosine triphosphatases, and growth factor receptors.[17–20] Caveolar membranes are also enriched in cholesterol, glycosphingolipids, and signaling enzymes, such as Src kinase.[21] In addition, caveolae are reported to respond to cell stretch and to contribute to stretch-induced signaling.[22] Integrins are reported to regulate multiple pathways, including ERK, PI3K, focal adhesion kinase (FAK), Src, and Rho guanosine triphosphatases.[23–25] Although caveolin-1 has no extracellular component, caveolin-1 may play an important role in sensing mechanical stress or the distortion of the extracellular membranes through interaction with β1-integrin.[19,20,26,27] In the present study, we aimed to demonstrate whether the LIPUS ameliorates post-MI LV remodeling and if so, to elucidate the underlying molecular mechanisms involved in the beneficial effects of the LIPUS.

Materials and Methods

Materials and Methods are available in the online-only Data Supplement.

Results

Effects of the LIPUS Therapy on Post-MI LV Remodeling In Vivo

To test whether the LIPUS therapy ameliorates LV dysfunction after AMI, wild-type mice were subjected to left anterior descending coronary artery ligation, and cardiac function was followed up for 2 months (Figure 1A). Mortality was significantly lower in the LIPUS group than in the no-LIPUS group (Figure 1B). In the no-LIPUS group, LV contractile function was progressively depressed 8 weeks after AMI, which was significantly ameliorated in the LIPUS group (fractional shortening at 8 weeks, 4.8±2.1% versus 12.7±1.6%; $P<0.01$; $P<0.0001$ by 2-way ANOVA; Figure 1C). In contrast, LIPUS therapy had no effects on cardiac function in the sham-operated animals (Figure 1C). Similarly, no difference in body weight or LV wall thickness was noted among the 4 groups during the study period (Figure IC in the online-only Data Supplement). Infarct size was significantly smaller in the MI-LIPUS group than in the MI-no-LIPUS group (Figure 1D). No complications, such as arrhythmias or skin burn, were noted during or after the treatment.

Effects of the LIPUS Therapy on Capillary Density and Signaling Pathways in the Infarcted Hearts In Vivo

Heart weight/tibia length ratio was significantly lower in the MI-LIPUS group than in the MI-no-LIPUS group on day 28 (Figure IIA in the online-only Data Supplement). Although there was no difference in capillary density on day 3 or day 6 between the 2 groups (Figure IIB in the online-only Data Supplement), capillary density in the border area on day 28 was significantly higher in the LIPUS group than in the no-LIPUS group (Figure 2A). There was no significant difference in heart weight/tibia length ratio or capillary density in the LV between the 2 groups on day 56. We then aimed to elucidate the molecular mechanisms involved in the beneficial effects of the LIPUS therapy. First, we examined the expression of angiogenic molecules in the infarcted, border, and remote areas of the LV in mice in vivo. mRNA expression of vascular endothelial growth factor (VEGF) and endothelial nitric oxide synthase (eNOS) in the infarcted area was upregulated in the LIPUS group compared with the no-LIPUS group on day 6, but not on day 3 (Figure 2B). Although mRNA expression of transforming growth factor-β1 was enhanced in the infarcted area, there was no difference in the expression levels between the MI-no-LIPUS and the MI-LIPUS groups (Figure IIC in the online-only Data Supplement). We also examined protein levels of VEGF, eNOS, and caveolin-1 and the extent of phosphorylation of extracellular signal-regulated kinase 1/2 (ERK1/2) and Akt (Figure 2C and 2D). In the infarcted area, the LIPUS therapy upregulated the expression of VEGF and eNOS on day 6, but not on days 3 and 28 (Figure 2C). The LIPUS therapy also enhanced phosphorylation of ERK1/2 (Thr202-Tyr204) and Akt (Ser473; Figure 2D). We also found that expression of caveolin-1 was significantly upregulated in the remote area on day 3, but not on day 6 or 28 (Figure IID in the online-only Data Supplement).

Effects of the LIPUS Therapy on Signaling Pathways in Human Umbilical Vein Endothelial Cells In Vitro

We then aimed to further elucidate the underlying molecular mechanisms involved in the beneficial effects of the LIPUS therapy in human umbilical vein endothelial cells (HUVECs) in vitro. First, we performed scratch assay to study the effects of the LIPUS on proliferation of HUVECs. The LIPUS significantly enhanced endothelial proliferation (Figure IIIB in the online-only Data Supplement). We confirmed that the LIPUS (for 20 minutes) upregulated the mRNA expression of VEGF with a peak at 6 hours after irradiation (6 hours, 1.42±0.28-fold versus controls; $P<0.05$; Figure 3A; Figure IIIC in the online-only Data Supplement). And, the mRNA expression level of caveolin-1 was correlated to that of VEGF in HUVECs 6 hours after LIPUS irradiation (Figure 3A). The LIPUS did not affect the expression of VEGF in human cardiac fibroblasts, whereas it slightly enhanced

Downloaded from http://atvb.ahajournals.org/ by guest on February 21, 2017

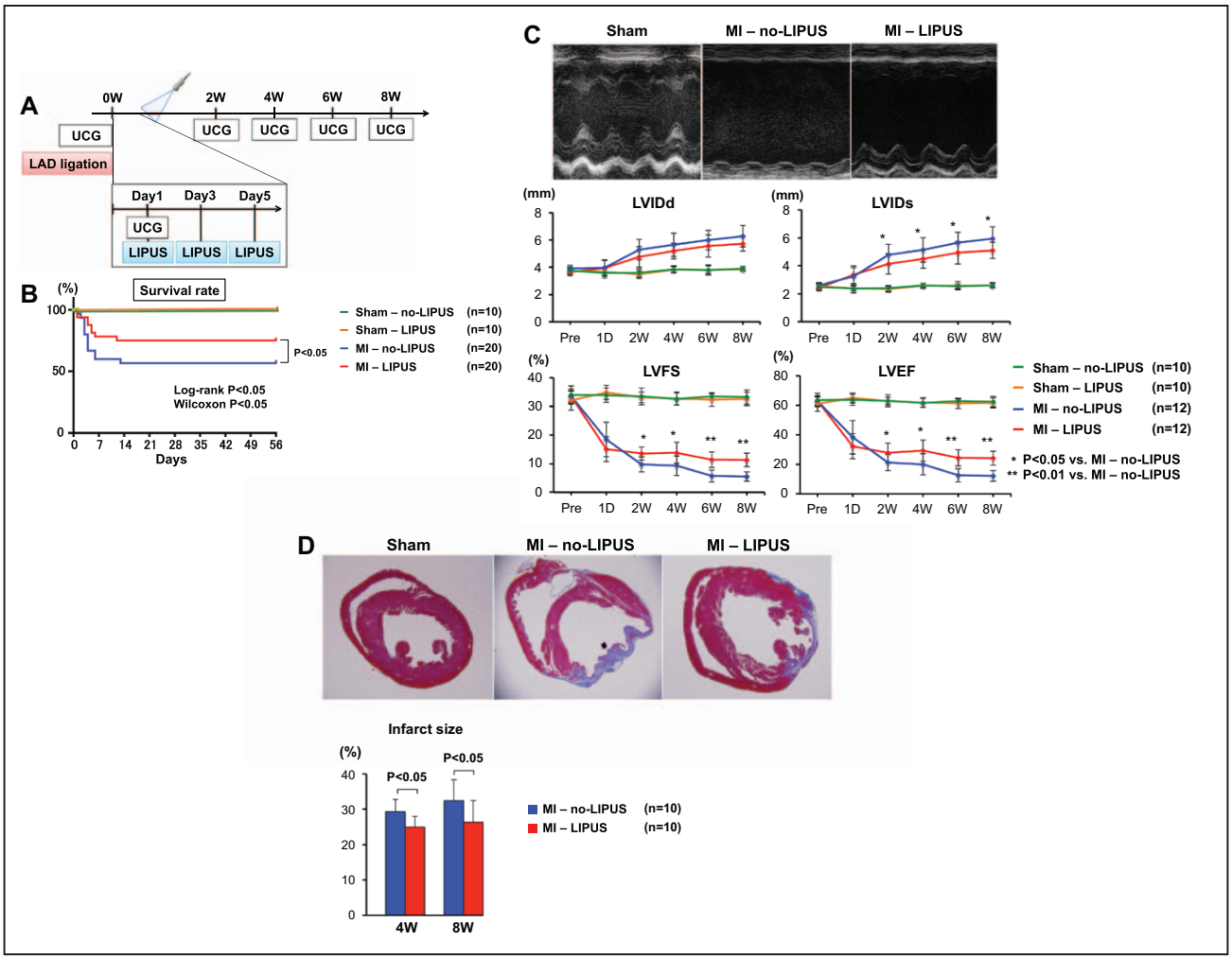

Figure 1. Low-intensity pulsed ultrasound (LIPUS) therapy ameliorates post–myocardial infarction (MI) left ventricular (LV) remodeling in mice in vivo. **A**, Study protocol. **B**, Survival rate. **C**, Representative M-mode echocardiographic images 8 wk after acute myocardial infarction. Graphs showing the time course of LV internal dimension at end diastole (LVIDd), LVID at end systole (LVIDs), LV fractional shortening (LVFS), and LV ejection fraction (LVEF). **D**, Representative photographs of heart sections stained with Masson trichrome staining on day 28. A graph shows the infarct size. Results are expressed as mean±SD. LAD indicates left anterior descending coronary artery; and UCG, ultrasoundcardiography.

the expression of VEGF in human cardiac myocytes (24 hours, 1.16±0.13-fold versus controls; $P<0.05$; Figure 3A). The protein expression of VEGF was enhanced at 24 hours after irradiation in the LIPUS group when compared with the control group (Figure 3B). Microarray analysis was performed in the harvested HUVECs and human coronary artery endothelial cells 6 hours after irradiation. In HUVECs, 31 385 probe sets were analyzed, where 1260 genes were found to be differentially expressed (upregulation in 224 gens and downregulation in 1036 genes). In human coronary artery endothelial cells, 31 710 probe sets were analyzed, where 1003 genes were found to be differentially expressed (upregulation in 381 genes and downregulation in 622 genes). We also analyzed the pooled data of HUVECs and human coronary artery endothelial cells after revising with ComBat analysis to eliminate the batch effects between the 2 cell types.[28] The ComBat analysis showed that a total of 1050 genes, including those of the VEGF signaling and focal adhesion pathways, were significantly altered by the LIPUS treatment (Figure 3C; Table II in the online-only Data Supplement). The data analyzed by Ingenuity Pathway Analysis tools (Ingenuity Systems, Mountain View, CA) represent the possible involvements of focal adhesion pathway and its downstream signaling pathways (Figure IIID in the online-only Data Supplement). Microarray analysis showed that the expression level of VEGF, eNOS, β1-integrin–like protein, and SIRT1 significantly upregulated by the LIPUS treatment, whereas that of caveolin-1 and β1-integrin unchanged (Figure IIIE in the online-only Data Supplement). To examine the role of focal adhesion pathway in the LIPUS-induced angiogenesis, we preformed studies with small interfering RNA (siRNA) to interfere some molecules that are supposed to be involved in the mechanotransduction cascade. Knockdown with siRNA of either β1-integrin or caveolin-1, both of which are known to play key roles in the mechanotransduction,[16,21–24] suppressed the LIPUS-induced upregulation of VEGF (Figure 3D). Knockdown with siRNA of either Fyn or FAK also suppressed the LIPUS-induced upregulation of VEGF (Figure 3D). To evaluate the importance of structure of caveolae itself, conformational changes of caveolae were induced with either knockdown of serum deprivation

Downloaded from http://atvb.ahajournals.org/ by guest on February 21, 2017

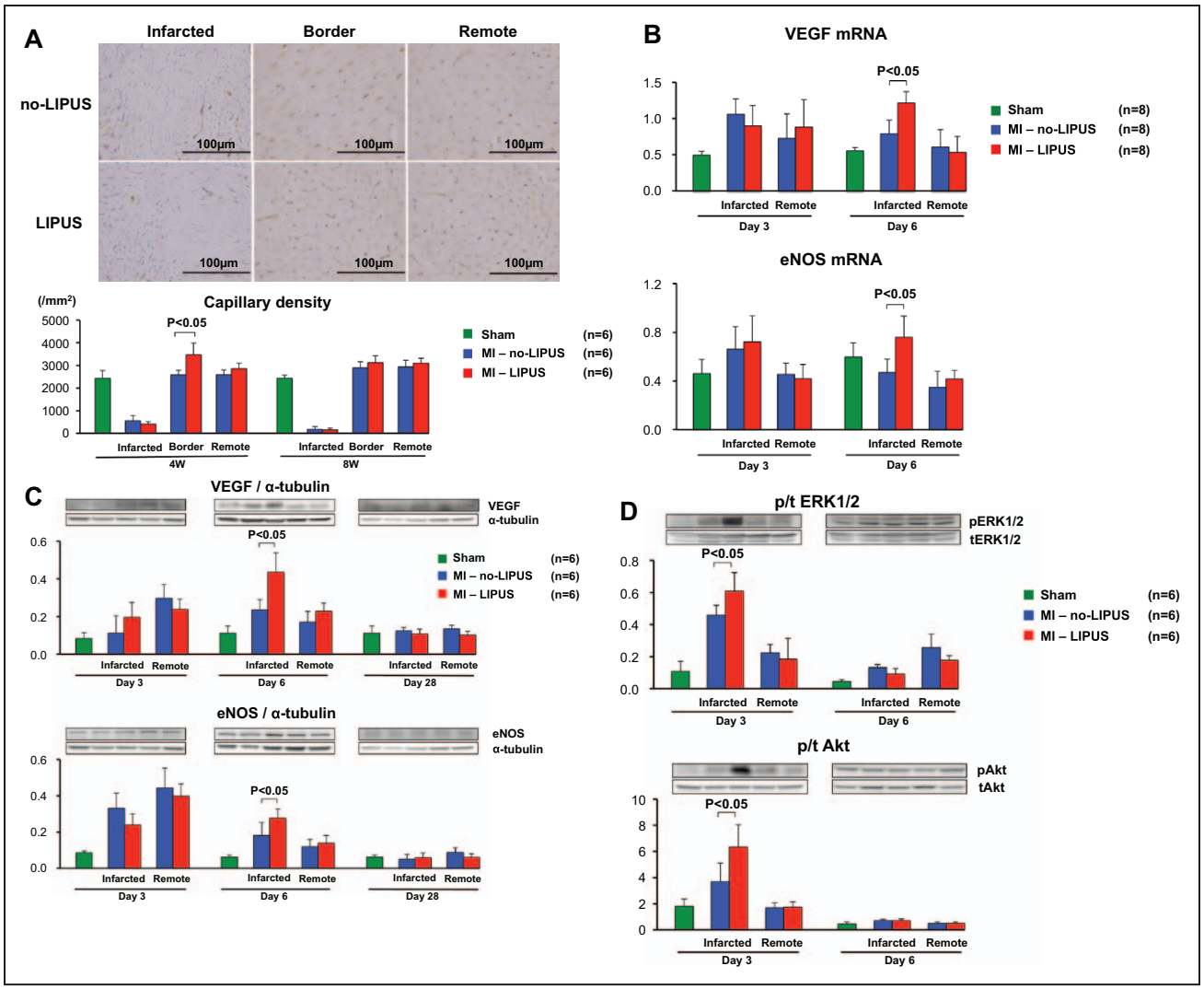

Figure 2. Low-intensity pulsed ultrasound (LIPUS) therapy enhances angiogenesis in the border area and upregulates vascular endothelial growth factor (VEGF) and endothelial nitric oxide synthase (eNOS) signaling pathways via phosphorylation of extracellular signal-regulated kinase 1/2 (ERK1/2) and Akt in the left ventricle in mice in vivo. **A**, Representative images of CD31 staining at day 28. Capillary density evaluated by CD31 staining. **B**, mRNA expression of VEGF and eNOS. **C**, Protein levels of VEGF and eNOS. **D**, Phosphorylation of ERK1/2 at Thr202-Tyr204 and Akt at Ser473. Results are expressed as mean±SD. MI indicates myocardial infarction; pAkt, phosphorylated Akt; and pERK, phosphorylated ERK.

response protein, a caveolar protein required for the formation of characteristic flask-shaped caveolar membrane invaginations, or methyl-β-cyclodextrin, an inhibitor specifically designed to disrupt lipid rafts in cells by depleting the cholesterol component.[29,30] Knockdown with siRNA of serum deprivation response protein suppressed the LIPUS-induced upregulation of VEGF (Figure 3D). In the cell lysate treated with methyl-β-cyclodextrin 30 minutes before irradiation, the LIPUS-induced upregulation of VEGF was also suppressed (Figure 3D). Knockdown with siRNA of each molecule was confirmed with real-time polymerase chain reaction (Figure IV in the online-only Data Supplement).

Effects of the LIPUS Therapy on Protein Phosphorylation in HUVEC In Vitro

To further examine the intracellular responses induced by the LIPUS, a comprehensive screening of protein phosphorylation was performed using the Bio-Plex system in HUVECs (Figure 4A; Figure VA in the online-only Data Supplement). Immediately after the LIPUS irradiation, phosphorylation of ERK1/2 (Thr202-Tyr204) and Akt (Ser473) was significantly enhanced in the LIPUS group compared with the control (no-LIPUS) group (Figure 4B). Phosphorylation of FAK (Tyr397), but not that of Fyn, was also significantly higher in the LIPUS group than in the control group (Figure 4B). The LIPUS did not enhance HUTS-4 expression in HUVECs, suggesting that the LIPUS has no significant effects on the activation state of β1-integrin (Figure VB in the online-only Data Supplement).[31] To further examine the involvement of each molecule in focal adhesion pathway, siRNA interference studies were performed. Knockdown with siRNA of either β1-integrin or caveolin-1 suppressed the LIPUS-induced phosphorylation of ERK1/2 and Akt (Figure 4C and 4D). Knockdown with siRNA of either Fyn or FAK also

Downloaded from http://atvb.ahajournals.org/ by guest on February 21, 2017

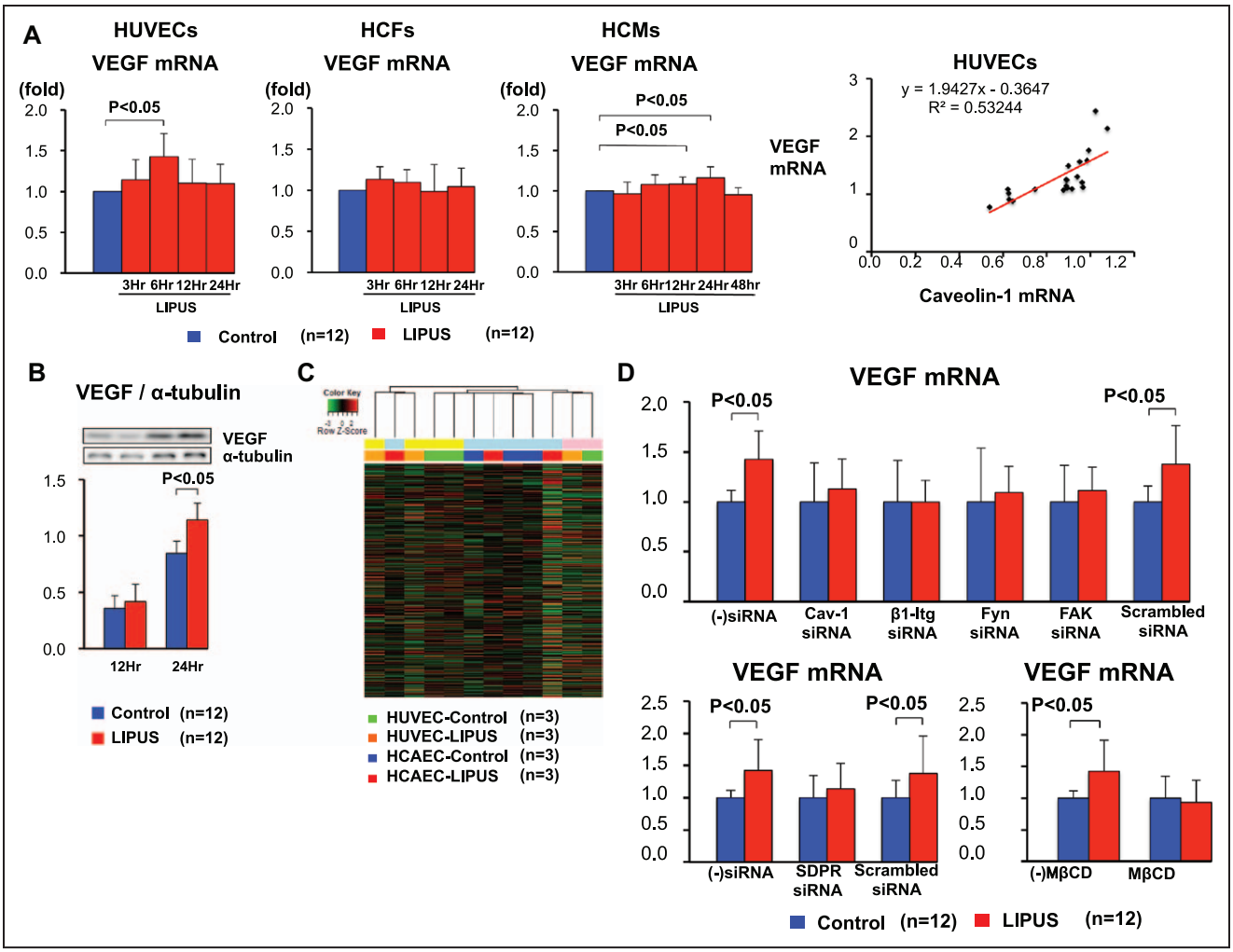

Figure 3. Focal adhesion pathway is crucial for the low-intensity pulsed ultrasound (LIPUS)–induced upregulation of vascular endothelial growth factor (VEGF) in vitro. **A**, mRNA expression of VEGF in human umbilical vein endothelial cells (HUVECs), human cardiac fibroblasts (HCFs), and human cardiac myocytes (HCMs) in response to LIPUS. And, a positive correlation between caveolin-1 (Cav-1) mRNA expression and VEGF mRNA expression in vitro. **B**, Protein levels of VEGF at 12 and 24 h after LIPUS irradiation. **C**, Heat map of the microarray clustering analysis of LIPUS-irradiated HUVECs and human coronary artery endothelial cells. **D**, Effects of knockdown of Cav-1, β1-integrin (β1-Itg), Fyn, and FAK with small interfering RNA (siRNA) on VEGF expression. Effects of knockdown of serum deprivation response protein (SDPR) with siRNA on VEGF expression. Effects of methyl-β-cyclodextrin (MβCD) on VEGF expression. The samples used for the analysis were HUVECs harvested 6 h after the LIPUS irradiation. Results are expressed as mean±SD.

suppressed the LIPUS-induced phosphorylation of ERK1/2 and Akt (Figure 4C and 4D). Knockdown of each molecule with siRNA was confirmed with Western blotting (Figure VC in the online-only Data Supplement).

Effects of the LIPUS Therapy on Post-MI LV Remodeling in Caveolin-1 Knockout Mice In Vivo

To confirm the contribution of caveolin-1 to the LIPUS-induced beneficial effects on post-MI LV remodeling in vivo, we examined the effects of the LIPUS therapy in caveolin-1 knockout (Cav-1-KO) mice. Cav-1-KO mice were subjected to left anterior descending coronary artery ligation and were treated with the LIPUS therapy. Unlike in wild-type mice (Figure 1B), the LIPUS therapy had no beneficial effects on the mortality in Cav-1-KO mice (Figure 5A). Similarly, the beneficial effects of the LIPUS therapy on contractile function, infarct size, and capillary density noted in wild-type mice were all absent in Cav-1-KO mice (Figure 5B–5D; Figure VI in the online-only Data Supplement). Furthermore, the LIPUS-induced upregulation of VEGF and eNOS mRNA expression and phosphorylation of ERK1/2 and Akt noted in wild-type mice were absent in Cav-1-KO mice (Figure VII in the online-only Data Supplement). The LIPUS-induced upregulation of VEGF and eNOS and LIPUS-enhanced phosphorylation of ERK1/2 and Akt were all blunted in endothelial cell–specific Cav-1-KO mice as in systemic Cav-1-KO mice (Figure VIII in the online-only Data Supplement). These results suggest that caveolin-1 plays a pivotal role in the beneficial effects of LIPUS on post-MI LV remodeling in mice in vivo.

Expression of Caveolin-1 in MI Mice and in Human Autopsy Samples

Immunohistochemical staining showed that the immunoreactivity of caveolin-1 was enhanced in the infarcted area

Downloaded from http://atvb.ahajournals.org/ by guest on February 21, 2017

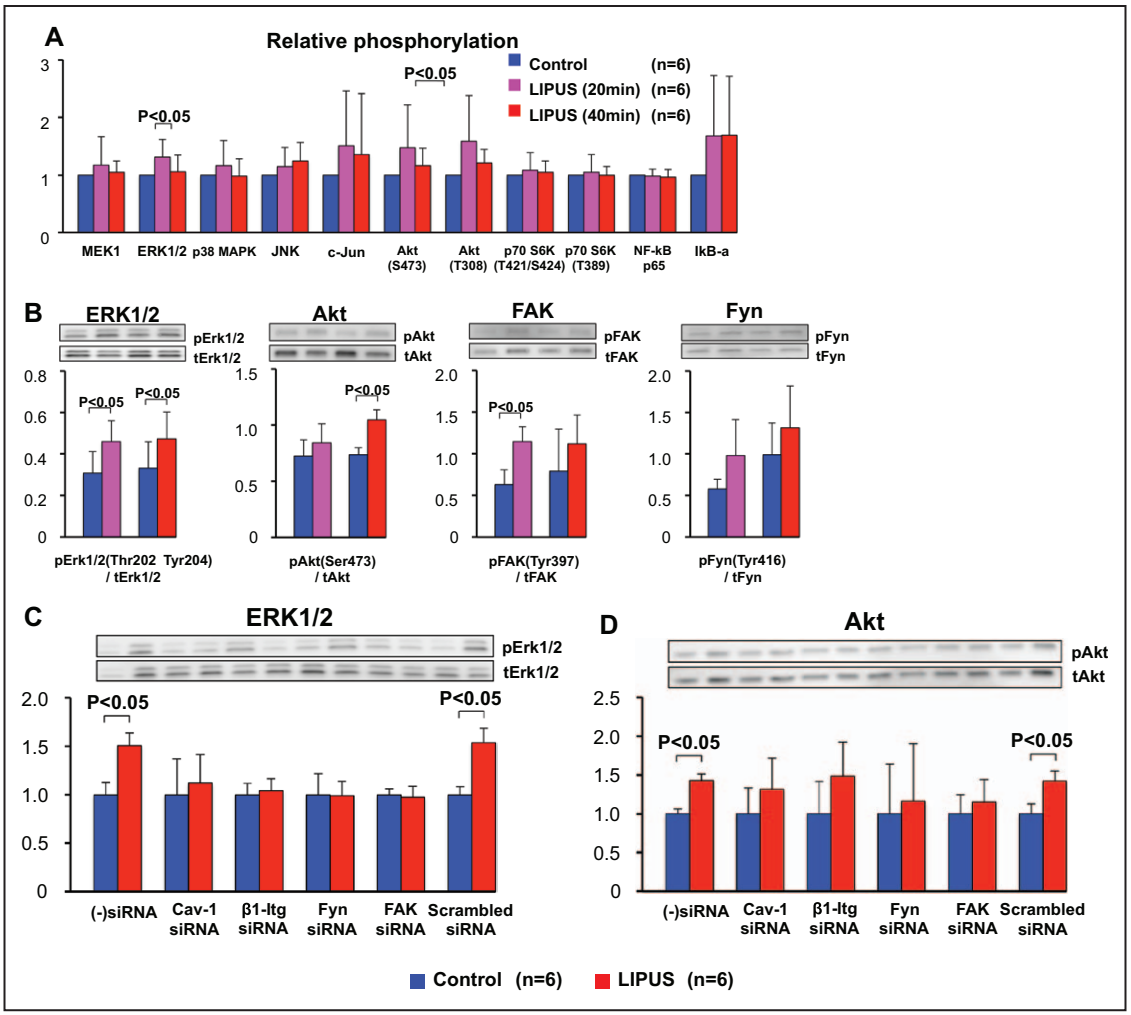

Figure 4. Low-intensity pulsed ultrasound (LIPUS) enhances extracellular signal-regulated kinase 1/2 (ERK1/2) and Akt phosphorylation in a focal adhesion pathway–dependent manner in vitro. **A**, The phosphoprotein assay with Bio-Plex in LIPUS-irradiated human umbilical vein endothelial cells. **B**, Phosphorylation of ERK1/2 at Thr202-Tyr204, Akt at Ser473, focal adhesion kinase (FAK) at Tyr397, and Fyn (Src) at Tyr416. Knockdown with small interfering RNA (siRNA) of caveolin-1 (Cav-1), β1-integrin (β1-Itg), Fyn, and FAK suppressed the LIPUS-induced ERK1/2 and Akt phosphorylation. **C**, Effects of knockdown of Cav-1, β1-Itg, Fyn, and FAK with siRNA on ERK1/2 at Thr202-Tyr204. **D**, Effects of knockdown with siRNA on Akt at Ser473. Results are expressed as mean±SD. MEK1 indicates MAPK kinase; and pAkt, phosphorylated Akt.

when compared with the remote area on day 3 in mice in vivo (Figure IX in the online-only Data Supplement). We also examined the expression of caveolin-1 in autopsy samples from patients who died of AMI. The immunoreactivity of caveolin-1 was significantly enhanced in coronary arterial endothelial cells in the ischemic myocardium (the distal site of the culprit coronary lesion) when compared with the remote area (Figure 6A–6C).

Discussion

In the present study, we were able to demonstrate that the LIPUS therapy ameliorates post-MI LV remodeling in mice in vivo, where the mechanotransduction system, including β1-integrin and caveolin-1 and its downstream pathways, plays pivotal roles in the beneficial effects of the LIPUS (Figure 6D). This study demonstrates the beneficial effects of the LIPUS therapy on post-MI LV remodeling and its intracellular signaling pathways.

Beneficial Effects of the LIPUS Therapy on Post-MI LV Remodeling in Mice In Vivo

In the present study, the LIPUS therapy enhanced angiogenesis, ameliorated post-MI LV remodeling, and improved the mortality in mice in vivo. We treated the animals with the LIPUS on days 1, 3, and 5, resulting in the enhanced phosphorylation of ERK1/2 and Akt on day 3 and the upregulation of VEGF and eNOS on day 6. Although the LIPUS therapy was performed only in the acute phase with resultant upregulation of VEGF and eNOS, capillary density was enhanced, and post-MI LV remodeling was ameliorated in the chronic phase. These results suggest that it is important to turn on the angiogenic pathways immediately after the onset of AMI to suppress post-MI LV remodeling. In the present study, the upregulation of VEGF in response to the LIPUS was prolonged as it was noted at day 6. We consider that the prolonged upregulation of VEGF was caused by the repetitive LIPUS treatment because we applied the LIPUS to the heart at 1, 3, and 5 days after MI.

Downloaded from http://atvb.ahajournals.org/ by guest on February 21, 2017

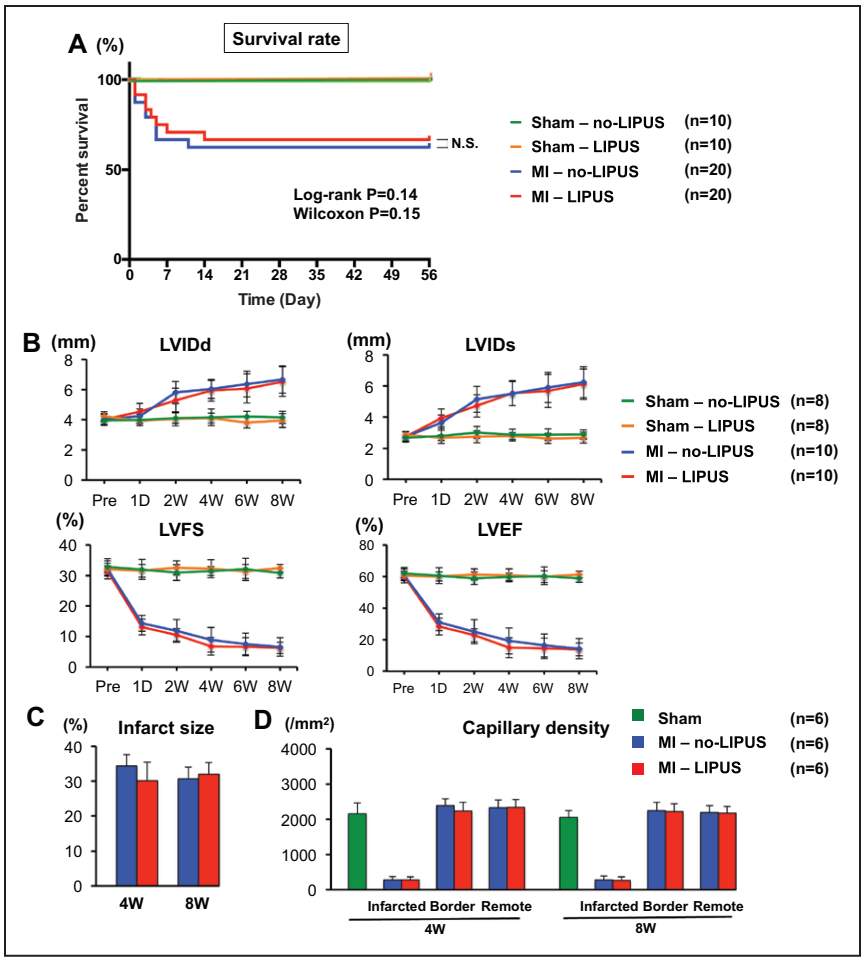

Figure 5. Absence of the beneficial effects of low-intensity pulsed ultrasound (LIPUS) on post–myocardial infarction (MI) left ventricular (LV) remodeling in caveolin-1 knockout mice. **A**, Survival rate. **B**, Echocardiographic evaluation. Graph showing the time course of LV internal dimension at end diastole (LVIDd), LVID at end systole (LVIDs), LV fractional shortening (LVFS), and LV ejection fraction (LVEF). **C**, Infarct size. **D**, Capillary density. Results are expressed as mean±SD.

Potential Mechanisms for Anginogenic Effects of the LIPUS Therapy After AMI

The degree of the LIPUS-induced upregulation of mRNA was higher in HUVECs than in human cardiac myocytes, suggesting that vascular endothelial cells may be the main player for the LIPUS-induced angiogenesis (Figure 3A). We performed comprehensive analysis of phosphorylation of angiogenesis-related proteins in HUVECs using the Bio-Plex phosphoprotein assay. In this analysis, phosphorylation of ERK1/2 and Akt was enhanced by the LIPUS therapy in vitro. The LIPUS therapy also enhanced the expression of VEGF and eNOS, followed by enhanced phosphorylation of ERK1/2 and Akt in the acute phase of AMI. Capillary density was higher in the LIPUS group than in the no-LIPUS group in the chronic phase. Microarray analysis showed that not only VEGF signaling pathway but also focal adhesion pathway was significantly affected by the LIPUS. Focal adhesion pathway contains several proteins on the cell membrane, including caveolin-1 and β1-integrin, both of which are important components of the caveolae and are known to play key roles in the mechanotransduction process.[15,16] Especially, caveolin-1 is required to maintain the structure of caveolae.[15,16] The present results with siRNA suggest that caveolin-1, β1-integrin, Fyn, FAK, ERK1/2, and Akt are all involved in the LIPUS-induced upregulation of VEGF (Figure 6D). In addition, we found that the conformational changes of caveolae by either knockdown of serum deprivation protein response with siRNA or administration of methyl-β-cyclodextrin suppressed the LIPUS-induced upregulation of VEGF. Furthermore, we demonstrated that the beneficial effects of the LIPUS therapy on post-MI LV remodeling were blunted in Cav-1-KO mice. LIPUS-induced upregulation of angiogenic molecules was also blunted in the endothelial cell–specific caveolin-1 knockout mice, suggesting that endothelial cells play pivotal roles in the angiogenic effects of the LIPUS. Taken together, these results suggest that the acoustic streaming by the LIPUS induces distortion of caveolae on endothelial cells, which then transmits the mechanical stimuli to intracellular signaling pathways with subsequent phosphorylation of Fyn, FAK, ERK1/2, and Akt and resultant enhanced the expression of VEGF and angiogenesis (Figure 6D). These molecules are also known to play key roles in cell proliferation and angiogenesis induced by mechanical stimuli (eg, shear stress) on the surface of vascular endothelial cells.[15,19–22,24]

Biological Effects of LIPUS Other Than Angiogenesis

The microarray analysis suggested that the LIPUS exerts biological effects on cell cycles, metabolic pathways, RNA transport, DNA replication, mRNA surveillance, mismatch repair, and protein export in addition to its angiogenic

Downloaded from http://atvb.ahajournals.org/ by guest on February 21, 2017

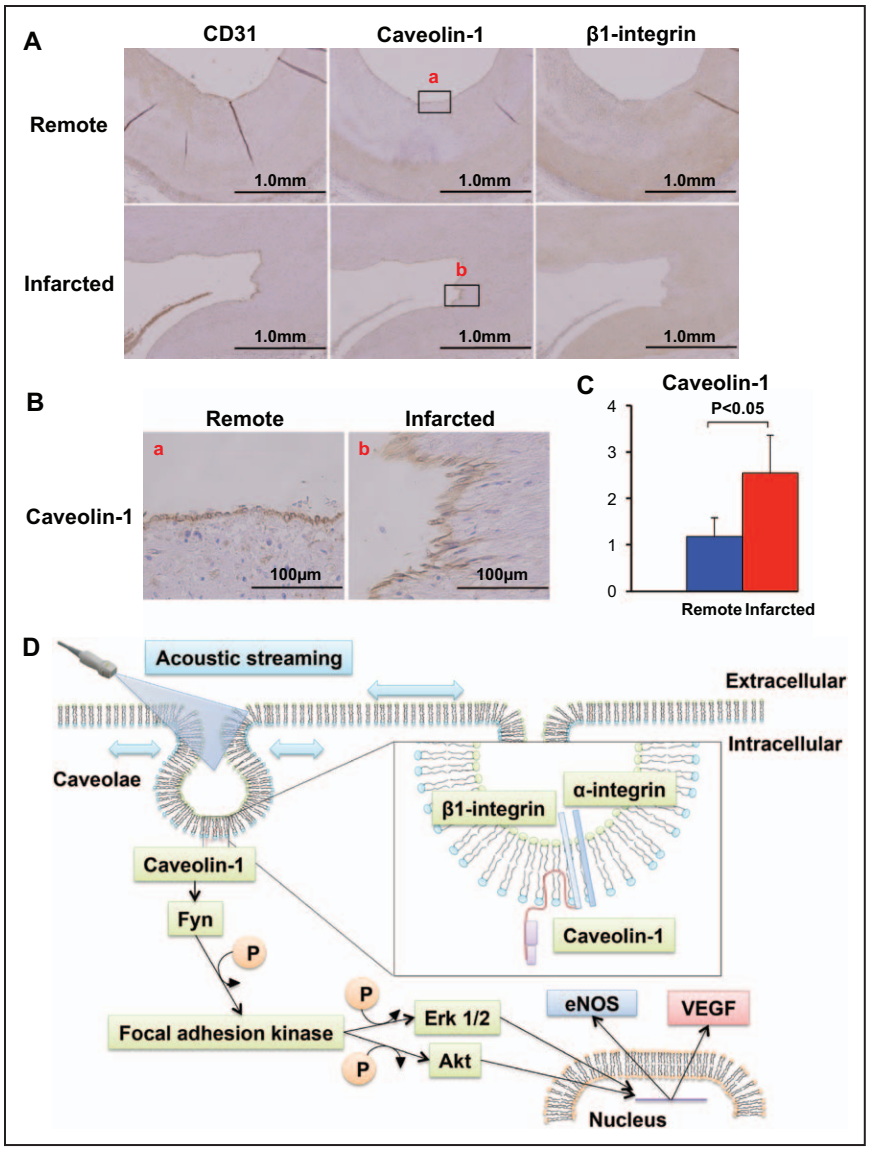

Figure 6. Expression of caveolin-1 in autopsy samples from patients with AMI and molecular mechanisms for the mechanotransduction in the low-intensity pulsed ultrasound (LIPUS)–induced angiogenesis. **A**, Representative images of immunostaining of CD31, caveolin-1, and β1-integrin in the infarcted and the remote areas. **B**, High-power fields of immunostaining of caveolin-1 from **A**. **C**, Expression of caveolin-1 by a semi-quantitative scoring system. **D**, Possible molecular mechanisms for the LIPUS-induced angiogenesis are shown. ERK1/2 indicates extracellular signal-regulated kinase 1/2; eNOS, endothelial nitric oxide synthase; and VEGF, vascular endothelial growth factor.

effects. In this regard, we have recently reported that the low-energy shock wave therapy suppresses post-MI LV remodeling in rats through anti-inflammatory effects in addition to its angiogenic effects,[32] suggesting that the LIPUS may also exert anti-inflammatory effects. Ultrasound has been reported to induce sonoporation and subsequent influx of calcium ion, which was correlated to the LIPUS-induced bioeffects in cultured cells.[33] Thus, it is possible that the LIPUS exerts several biological effects through alteration of intracellular Ca^{2+} levels. This point remains to be examined in future studies.

Role of Caveolin-1 in the Ischemic Heart

It is reported that the shear stress–induced intracellular signaling is mediated by the activation of β1-integrin and concurrent caveolin-1 phosphorylation.[34] β1-integrin–mediated activation of ERK1/2 and PI3-Akt pathways is mediated by caveolin-1.[35] In the present study, endothelial expression of caveolin-1 was enhanced in the infarcted area early after AMI in mice and in autopsy samples of patients with AMI, suggesting that the abrupt reduction of coronary flow and shear stress affects endothelial cells in the ischemic myocardium to upregulate caveolin-1, leading to an increased sensitivity to LIPUS.

Study Limitations

Several limitations should be mentioned for the present study. First, the effects of LIPUS on VEGF expression were rather small in in vitro studies compared with those observed in in vivo studies. In the present study, the LIPUS was applied to the cells for 20 minutes in in vitro studies, whereas it was applied to the heart at 3 different short-axis levels on 1, 3, and 5 days after AMI in in vivo studies (20 minutes×3 levels×3 days). We speculate that the repeated irradiation enhanced the effects of LIPUS on angiogenesis. Second, it has been reported that Cav-1-KO mice develop cardiac hypertrophy and impaired coronary collateral growth in response to ischemia.[36] Thus, the beneficial effects of

Downloaded from http://atvb.ahajournals.org/ by guest on February 21, 2017

LIPUS might be further blunted in Cav-1-KO mice. Third, we did not examine the effects of the LIPUS in genetically modified animals other than Cav-1-KO mice because β1-integrin knockout mice are embryonic lethal.[37] Fourth, about the molecular mechanisms for the LIPUS-induced angiogenic effects, we focused on focal adhesion pathway in the present study based on the results of microarray analysis. Although we showed that caveolin-1, β1-integrin, Fyn, and FAK play pivotal roles in the LIPUS-induced signaling pathway, other subcellular structures related to mechanotransduction, such as cytoskeleton and cell adhesion complexes, might also be involved.[38] Further studies are needed. Fifth, in the siRNA experiments, we used VEGF as an index of angiogenic effects of the LIPUS. However, it is possible that other mechanisms related to angiogenesis, such as anti-inflammatory and antifibrotic effects, may also contribute to the beneficial effects of the LIPUS. This point also remains to be examined in future studies.

Clinical Implications

Despite recent progress in emergency care and management of AMI, post-MI remodeling and heart failure remain an important issue in cardiovascular medicine.[1–3] Although regenerative therapies, such as gene and cell therapies, have been under development to suppress worsening heart failure,[39,40] most of them are invasive in nature, and their efficacy and safety have not been established yet.[41–43] Because the intensity of ultrasound used in the LIPUS therapy is below the upper limit of acoustic output standards for diagnostic ultrasound devices, the therapy does not cause compression, heat, or discomfort. For this noninvasive nature, our LIPUS therapy can be used as an adjunctive therapy in patients with AMI to suppress post-MI LV remodeling. It could also be applied to other ischemic disorders, such as ischemic cardiomyopathy, peripheral arterial disease, refractory chronic skin ulcers, and spinal cord injury as in the case with low-energy extracorporeal shock wave therapy.[44–46]

Conclusions

In the present study, we were able to demonstrate that the LIPUS therapy ameliorates post-MI LV remodeling in mice in vivo, where mechanotransduction and its downstream pathways may be involved. Thus, the LIPUS therapy may be a promising, new, noninvasive strategy for the treatment of post-MI LV remodeling.

Acknowledgments

We thank Yumi Watanabe, Ai Nishihara, and Hiromi Yamashita for their excellent technical assistance.

Sources of Funding

This study was supported in part by Grants-in-Aid for Scientific Research from the Japanese Ministry of Education, Culture, Sports, Science, and Technology, Tokyo, Japan, and the Japanese Ministry of Health, Labor, and Welfare, Tokyo, Japan.

Disclosures

None.

References

1. Moran AE, Forouzanfar MH, Roth GA, Mensah GA, Ezzati M, Murray CJ, Naghavi M. Temporal trends in ischemic heart disease mortality in 21 world regions, 1980 to 2010: the Global Burden of Disease 2010 study. *Circulation*. 2014;129:1483–1492. doi: 10.1161/CIRCULATIONAHA.113.004042.
2. O'Gara PT, Kushner FG, Ascheim DD, et al; American College of Cardiology Foundation/American Heart Association Task Force on Practice Guidelines. 2013 ACCF/AHA guideline for the management of ST-elevation myocardial infarction: a report of the American College of Cardiology Foundation/American Heart Association Task Force on Practice Guidelines. *Circulation*. 2013;127:e362–e425. doi: 10.1161/CIR.0b013e3182742cf6.
3. Windecker S, Kolh P, Alfonso F, et al. 2014 ESC/EACTS guidelines on myocardial revascularization: The Task Force on Myocardial Revascularization of the European Society of Cardiology (ESC) and the European Association for Cardio-Thoracic Surgery (EACTS) Developed with the special contribution of the European Association of Percutaneous Cardiovascular Interventions (EAPCI). *Eur Heart J*. 2014;35:2541–2619. doi: 10.1093/ejcts/ezu366.
4. Nishida T, Shimokawa H, Oi K, Tatewaki H, Uwatoku T, Abe K, Matsumoto Y, Kajihara N, Eto M, Matsuda T, Yasui H, Takeshita A, Sunagawa K. Extracorporeal cardiac shock wave therapy markedly ameliorates ischemia-induced myocardial dysfunction in pigs in vivo. *Circulation*. 2004;110:3055–3061. doi: 10.1161/01.CIR.0000148849.51177.97.
5. Fukumoto Y, Ito A, Uwatoku T, Matoba T, Kishi T, Tanaka H, Takeshita A, Sunagawa K, Shimokawa H. Extracorporeal cardiac shock wave therapy ameliorates myocardial ischemia in patients with severe coronary artery disease. *Coron Artery Dis*. 2006;17:63–70.
6. Kikuchi Y, Ito K, Ito Y, Shiroto T, Tsuburaya R, Aizawa K, Hao K, Fukumoto Y, Takahashi J, Takeda M, Nakayama M, Yasuda S, Kuriyama S, Tsuji I, Shimokawa H. Double-blind and placebo-controlled study of the effectiveness and safety of extracorporeal cardiac shock wave therapy for severe angina pectoris. *Circ J*. 2010;74:589–591.
7. Ito K, Fukumoto Y, Shimokawa H. Extracorporeal shock wave therapy for ischemic cardiovascular disorders. *Am J Cardiovasc Drugs*. 2011;11:295–302. doi: 10.2165/11592760-000000000-00000.
8. Hanawa K, Ito K, Aizawa K, Shindo T, Nishimiya K, Hasebe Y, Tuburaya R, Hasegawa H, Yasuda S, Kanai H, Shimokawa H. Low-intensity pulsed ultrasound induces angiogenesis and ameliorates left ventricular dysfunction in a porcine model of chronic myocardial ischemia. *PLoS One*. 2014;9:e104863. doi: 10.1371/journal.pone.0104863.
9. Barzelai S, Sharabani-Yosef O, Holbova R, Castel D, Walden R, Engelberg S, Scheinowitz M. Low-intensity ultrasound induces angiogenesis in rat hind-limb ischemia. *Ultrasound Med Biol*. 2006;32:139–145. doi: 10.1016/j.ultrasmedbio.2005.08.010.
10. Ramli R, Reher P, Harris M, Meghji S. The effect of ultrasound on angiogenesis: an *in vivo* study using the chick chorioallantoic membrane. *Int J Oral Maxillofac Implants*. 2009;24:591–596.
11. Martinez de Albornoz P, Khanna A, Longo UG, Forriol F, Maffulli N. The evidence of low-intensity pulsed ultrasound for in vitro, animal and human fracture healing. *Br Med Bull*. 2011;100:39–57. doi: 10.1093/bmb/ldr006.
12. Tanaka E, Kuroda S, Horiuchi S, Tabata A, El-Bialy T. Low-intensity pulsed ultrasound in dentofacial tissue engineering. *Ann Biomed Eng*. 2015;43:871–886. doi: 10.1007/s10439-015-1274-y.
13. Yang FY, Lu WW, Lin WT, Chang CW, Huang SL. Enhancement of neurotrophic factors in astrocyte for neuroprotective effects in brain disorders using low-intensity pulsed ultrasound stimulation. *Brain Stimul*. 2015;8:465–473. doi: 10.1016/j.brs.2014.11.017.
14. Mizrahi N, Seliktar D, Kimmel E. Ultrasound-induced angiogenic response in endothelial cells. *Ultrasound Med Biol*. 2007;33:1818–1829. doi: 10.1016/j.ultrasmedbio.2007.05.007.
15. Parton RG. Cell biology. Life without caveolae. *Science*. 2001;293:2404–2405. doi: 10.1126/science.1065677.
16. Parton RG, del Pozo MA. Caveolae as plasma membrane sensors, protectors and organizers. *Nat Rev Mol Cell Biol*. 2013;14:98–112. doi: 10.1038/nrm3512.
17. Sedding DG, Hermsen J, Seay U, Eickelberg O, Kummer W, Schwencke C, Strasser RH, Tillmanns H, Braun-Dullaeus RC. Caveolin-1 facilitates mechanosensitive protein kinase B (Akt) signaling *in vitro* and *in vivo*. *Circ Res*. 2005;96:635–642. doi: 10.1161/01.RES.0000160610.61306.0f.
18. Sonveaux P, Martinive P, DeWever J, Batova Z, Daneau G, Pelat M, Ghisdal P, Grégoire V, Dessy C, Balligand JL, Feron O. Caveolin-1 expression

Downloaded from http://atvb.ahajournals.org/ by guest on February 21, 2017

is critical for vascular endothelial growth factor-induced ischemic hindlimb collateralization and nitric oxide-mediated angiogenesis. *Circ Res*. 2004;95:154–161. doi: 10.1161/01.RES.0000136344.27825.72.
19. del Pozo MA, Balasubramanian N, Alderson NB, Kiosses WB, Grande-García A, Anderson RG, Schwartz MA. Phospho-caveolin-1 mediates integrin-regulated membrane domain internalization. *Nat Cell Biol*. 2005;7:901–908. doi: 10.1038/ncb1293.
20. Jokhadar SZ, Majhenc J, Svetina S, Batista U. Positioning of integrin β1, caveolin-1 and focal adhesion kinase on the adhered membrane of spreading cells. *Cell Biol Int*. 2013;37:1276–1284. doi: 10.1002/cbin.10155.
21. Wary KK, Mariotti A, Zurzolo C, Giancotti FG. A requirement for caveolin-1 and associated kinase Fyn in integrin signaling and anchorage-dependent cell growth. *Cell*. 1998;94:625–634.
22. Yu J, Bergaya S, Murata T, Alp IF, Bauer MP, Lin MI, Drab M, Kurzchalia TV, Stan RV, Sessa WC. Direct evidence for the role of caveolin-1 and caveolae in mechanotransduction and remodeling of blood vessels. *J Clin Invest*. 2006;116:1284–1291. doi: 10.1172/JCI27100.
23. Salanueva IJ, Cerezo A, Guadamillas MC, del Pozo MA. Integrin regulation of caveolin function. *J Cell Mol Med*. 2007;11:969–980. doi: 10.1111/j.1582-4934.2007.00109.x.
24. Shyy JY, Chien S. Role of integrins in endothelial mechanosensing of shear stress. *Circ Res*. 2002;91:769–775.
25. Bock-Marquette I, Saxena A, White MD, Dimaio JM, Srivastava D. Thymosin beta4 activates integrin-linked kinase and promotes cardiac cell migration, survival and cardiac repair. *Nature*. 2004;432:466–472. doi: 10.1038/nature03000.
26. Yeo MG, Oh HJ, Cho HS, Chun JS, Marcantonio EE, Song WK. Phosphorylation of Ser 21 in Fyn regulates its kinase activity, focal adhesion targeting, and is required for cell migration. *J Cell Physiol*. 2011;226:236–247. doi: 10.1002/jcp.22335.
27. Gervásio OL, Phillips WD, Cole L, Allen DG. Caveolae respond to cell stretch and contribute to stretch-induced signaling. *J Cell Sci*. 2011;124(pt 21):3581–3590. doi: 10.1242/jcs.084376.
28. Stein CK, Qu P, Epstein J, Buros A, Rosenthal A, Crowley J, Morgan G, Barlogie B. Removing batch effects from purified plasma cell gene expression microarrays with modified ComBat. *BMC Bioinformatics*. 2015;16:63. doi: 10.1186/s12859-015-0478-3.
29. Hansen CG, Bright NA, Howard G, Nichols BJ. SDPR induces membrane curvature and functions in the formation of caveolae. *Nat Cell Biol*. 2009;11:807–814. doi: 10.1038/ncb1887.
30. Hill MM, Daud NH, Aung CS, Loo D, Martin S, Murphy S, Black DM, Barry R, Simpson F, Liu L, Pilch PF, Hancock JF, Parat MO, Parton RG. Co-regulation of cell polarization and migration by caveolar proteins PTRF/Cavin-1 and caveolin-1. *PLoS One*. 2012;7:e43041. doi: 10.1371/journal.pone.0043041.
31. Luque A, Gómez M, Puzon W, Takada Y, Sánchez-Madrid F, Cabañas C. Activated conformations of very late activation integrins detected by a group of antibodies (HUTS) specific for a novel regulatory region (355-425) of the common beta 1 chain. *J Biol Chem*. 1996;271:11067–11075.
32. Abe Y, Ito K, Hao K, Shindo T, Ogata T, Kagaya Y, Kurosawa R, Nishimiya K, Satoh K, Miyata S, Kawakami K, Shimokawa H. Extracorporeal low-energy shock-wave therapy exerts anti-inflammatory effects in a rat model of acute myocardial infarction. *Circ J*. 2014;78:2915–2925.
33. Hassan MA, Campbell P, Kondo T. The role of Ca(2+) in ultrasound-elicited bioeffects: progress, perspectives and prospects. *Drug Discov Today*. 2010;15:892–906. doi: 10.1016/j.drudis.2010.08.005.
34. Rizzo V, Sung A, Oh P, Schnitzer JE. Rapid mechanotransduction in situ at the luminal cell surface of vascular endothelium and its caveolae. *J Biol Chem*. 1998;273:26323–26329.
35. Echarri A, Del Pozo MA. Caveolae internalization regulates integrin-dependent signaling pathways. *Cell Cycle*. 2006;5:2179–2182.
36. Jasmin JF, Rengo G, Lymperopoulos A, Gupta R, Eaton GJ, Quann K, Gonzales DM, Mercier I, Koch WJ, Lisanti MP. Caveolin-1 deficiency exacerbates cardiac dysfunction and reduces survival in mice with myocardial infarction. *Am J Physiol Heart Circ Physiol*. 2011;300:H1274–H1281. doi: 10.1152/ajpheart.01173.2010.
37. Takada Y, Ye X, Simon S. The integrins. *Genome Biol*. 2007;8:215. doi: 10.1186/gb-2007-8-5-215.
38. Hoffman BD, Grashoff C, Schwartz MA. Dynamic molecular processes mediate cellular mechanotransduction. *Nature*. 2011;475:316–323. doi: 10.1038/nature10316.
39. Marshall E. Gene therapy death prompts review of adenovirus vector. *Science*. 1999;286:2244–2245.
40. Sekine H, Shimizu T, Hobo K, Sekiya S, Yang J, Yamato M, Kurosawa H, Kobayashi E, Okano T. Endothelial cell coculture within tissue-engineered cardiomyocyte sheets enhances neovascularization and improves cardiac function of ischemic hearts. *Circulation*. 2008;118(suppl 14):S145–S152. doi: 10.1161/CIRCULATIONAHA.107.757286.
41. Rosengart TK, Lee LY, Patel SR, et al. Angiogenesis gene therapy: phase I assessment of direct intramyocardial administration of an adenovirus vector expressing VEGF121 cDNA to individuals with clinically significant severe coronary artery disease. *Circulation*. 1999;100:468–474.
42. Menasché P, Alfieri O, Janssens S, McKenna W, Reichenspurner H, Trinquart L, Vilquin JT, Marolleau JP, Seymour B, Larghero J, Lake S, Chatellier G, Solomon S, Desnos M, Hagège AA. The Myoblast Autologous Grafting in Ischemic Cardiomyopathy (MAGIC) trial: first randomized placebo-controlled study of myoblast transplantation. *Circulation*. 2008;117:1189–1200. doi: 10.1161/CIRCULATIONAHA.107.734103.
43. Chachques JC, Trainini JC, Lago N, Cortes-Morichetti M, Schussler O, Carpentier A. Myocardial Assistance by Grafting a New Bioartificial Upgraded Myocardium (MAGNUM trial): clinical feasibility study. *Ann Thorac Surg*. 2008;85:901–908. doi: 10.1016/j.athoracsur.2007.10.052.
44. Serizawa F, Ito K, Kawamura K, Tsuchida K, Hamada Y, Zukeran T, Shimizu T, Akamatsu D, Hashimoto M, Goto H, Watanabe T, Sato A, Shimokawa H, Satomi S. Extracorporeal shock wave therapy improves the walking ability of patients with peripheral artery disease and intermittent claudication. *Circ J*. 2012;76:1486–1493.
45. Hayashi D, Kawakami K, Ito K, Ishii K, Tanno H, Imai Y, Kanno E, Maruyama R, Shimokawa H, Tachi M. Low-energy extracorporeal shock wave therapy enhances skin wound healing in diabetic mice: a critical role of endothelial nitric oxide synthase. *Wound Repair Regen*. 2012;20:887–895. doi: 10.1111/j.1524-475X.2012.00851.x.
46. Yamaya S, Ozawa H, Kanno H, Kishimoto KN, Sekiguchi A, Tateda S, Yahata K, Ito K, Shimokawa H, Itoi E. Low-energy extracorporeal shock wave therapy promotes vascular endothelial growth factor expression and improves locomotor recovery after spinal cord injury. *J Neurosurg*. 2014;121:1514–1525. doi: 10.3171/2014.8.JNS132562.This article was sent to Qingbo Xu, Consulting Editor, for review by expert referees, editorial decision, and final disposition.

Highlights

- The low-intensity pulsed ultrasound (LIPUS) therapy ameliorates post–myocardial infarction left ventricular remodeling in mice in vivo.
- The mechanotransduction system, including β1-integrin and caveolin-1 and its downstream pathways, plays pivotal roles in the beneficial effects of the LIPUS therapy.
- Our current study provides a promising, new, noninvasive strategy for the patients with acute myocardial infarction and also clarifies the importance of mechanotransduction.

Downloaded from http://atvb.ahajournals.org/ by guest on February 21, 2017

Arteriosclerosis, Thrombosis, and Vascular Biology

JOURNAL OF THE AMERICAN HEART ASSOCIATION

Downloaded from http://atvb.ahajournals.org/ by guest on February 21, 2017

Low-Intensity Pulsed Ultrasound Enhances Angiogenesis and Ameliorates Left Ventricular Dysfunction in a Mouse Model of Acute Myocardial Infarction

Tomohiko Shindo, Kenta Ito, Tsuyoshi Ogata, Kazuaki Hatanaka, Ryo Kurosawa, Kumiko Eguchi, Yuta Kagaya, Kenichiro Hanawa, Kentaro Aizawa, Takashi Shiroto, Sachie Kasukabe, Satoshi Miyata, Hirofumi Taki, Hideyuki Hasegawa, Hiroshi Kanai and Hiroaki Shimokawa

Arterioscler Thromb Vasc Biol. 2016;36:1220-1229; originally published online April 14, 2016;
doi: 10.1161/ATVBAHA.115.306477
Arteriosclerosis, Thrombosis, and Vascular Biology is published by the American Heart Association, 7272 Greenville Avenue, Dallas, TX 75231
Copyright © 2016 American Heart Association, Inc. All rights reserved.
Print ISSN: 1079-5642. Online ISSN: 1524-4636

The online version of this article, along with updated information and services, is located on the World Wide Web at:
http://atvb.ahajournals.org/content/36/6/1220

Data Supplement (unedited) at:
http://atvb.ahajournals.org/content/suppl/2016/04/13/ATVBAHA.115.306477.DC1
http://atvb.ahajournals.org/content/suppl/2016/04/13/ATVBAHA.115.306477.DC2

Permissions: Requests for permissions to reproduce figures, tables, or portions of articles originally published in *Arteriosclerosis, Thrombosis, and Vascular Biology* can be obtained via RightsLink, a service of the Copyright Clearance Center, not the Editorial Office. Once the online version of the published article for which permission is being requested is located, click Request Permissions in the middle column of the Web page under Services. Further information about this process is available in the Permissions and Rights Question and Answer document.

Reprints: Information about reprints can be found online at:
http://www.lww.com/reprints

Subscriptions: Information about subscribing to *Arteriosclerosis, Thrombosis, and Vascular Biology* is online at:
http://atvb.ahajournals.org//subscriptions/

SUPPLEMENTAL MATERIAL

Low-intensity Pulsed Ultrasound Enhances Angiogenesis and Ameliorates Left Ventricular Dysfunction in a Mouse Model of Acute Myocardial Infarction

Tomohiko Shindo,[1] Kenta Ito,[1] Tsuyoshi Ogata, [1] Kazuaki Hatanaka,[1] Ryo Kurosawa,[1] Kumiko Eguchi,[1] Yuta Kagaya,[1] Kenichiro Hanawa,[1] Kentaro Aizawa,[1] Takashi Shiroto,[1] Sachie Kasukabe,[1] Satoshi Miyata,[1] Hirofumi Taki,[2,3] Hideyuki Hasegawa,[2,3] Hiroshi Kanai,[2,3] Hiroaki Shimokawa.[1]

[1]Department of Cardiovascular Medicine, Tohoku University Graduate School of Medicine, Sendai, Japan, [2]Department of Electronic Engineering, Graduate School of Engineering, Tohoku University, Sendai, Japan, and [3]Division of Biomedical Measurements and Diagnostics, Graduate School of Biomedical Engineering, Tohoku University, Sendai, Japan.

Running title: LIPUS Ameliorates LV Dysfunction after AMI

Key words: angiogenesis, mechanotransduction, cell signaling, contractile reserve, infarct remodeling

Subject Codes: [27] Other Treatment, [105] Contractile function, [129] Angiogenesis, [138] Cell signaling/signal transduction, [151] Ischemic biology - basic studies.

TOC category: Basic study

TOC subcategory: Vascular Biology

Address for Correspondence:

Kenta Ito, MD, PhD.
Associate Professor
Department of Cardiovascular Medicine
Tohoku University Graduate School of Medicine
1-1 Seiryo-machi, Aoba-ku, Sendai 980-8574, Japan
TEL: +81-22-717-7153, FAX: +81-22-717-7156
E-mail: ito-kenta@cardio.med.tohoku.ac.jp

Supplemental Tables

Table I. List of Antibodies Used in the Present Study

Antibody	Application	Dilution	Company
VEGF	Immunoblot	1:1000	Santa Cruz#sc-152
eNOS	Immunoblot	1:1000	Enzo#ADI-905-386
HUTS-4	Immunoblot	1:1000	LSP#LS-B2861-50
α-tubulin	Immunoblot	1:1000	Sigma#T5168
Phospho-ERK1/2	Immunoblot	1:1000	Cell Signaling#9106
Total- ERK1/2	Immunoblot	1:1000	Cell Signaling#9102
Phospho-Akt	Immunoblot	1:1000	Cell Signaling#9271
Total-Akt	Immunoblot	1:1000	Cell Signaling#9272
Phospho-Src	Immunoblot	1:1000	Cell Signaling#6943
Total-Fyn	Immunoblot	1:1000	Cell Signaling#4023
Phospho-FAK	Immunoblot	1:1000	Cell Signaling#8556
Total-FAK	Immunoblot	1:1000	Cell Signaling#3285
Caveolin-1	Immunoblot	1:1000	Cell Signaling#3238
β1-integrin	Immunoblot	1:1000	Cell Signaling#4706
CD31	IP	1:1000	Dako#M0823
Caveolin-1	IP	1:400	Cell Signaling#3238
β1-integrin	IP	1:100	Cell Signaling#4706

Table II. Results of the Microarray Clustering Analysis of LIPUS-irradiated HUVECs and HCAECs

Signaling pathway	P value
Cell cycle	0.00001
Metabolic pathway	0.00001
RNA transport	0.00001
DNA replication	0.00001
mRNA surveillance pathway	0.00001
Mismatch repair	0.00001
VEGF signaling pathway	0.00001
Protein export	0.0005
Glutathione metabolism	0.0017
Notch signaling pathway	0.003
Focal adhesion	0.0049
Phosphatidylinositol signaling system	0.0117
GnRH signaling pathway	0.0177
ErbB signaling pathway	0.0201

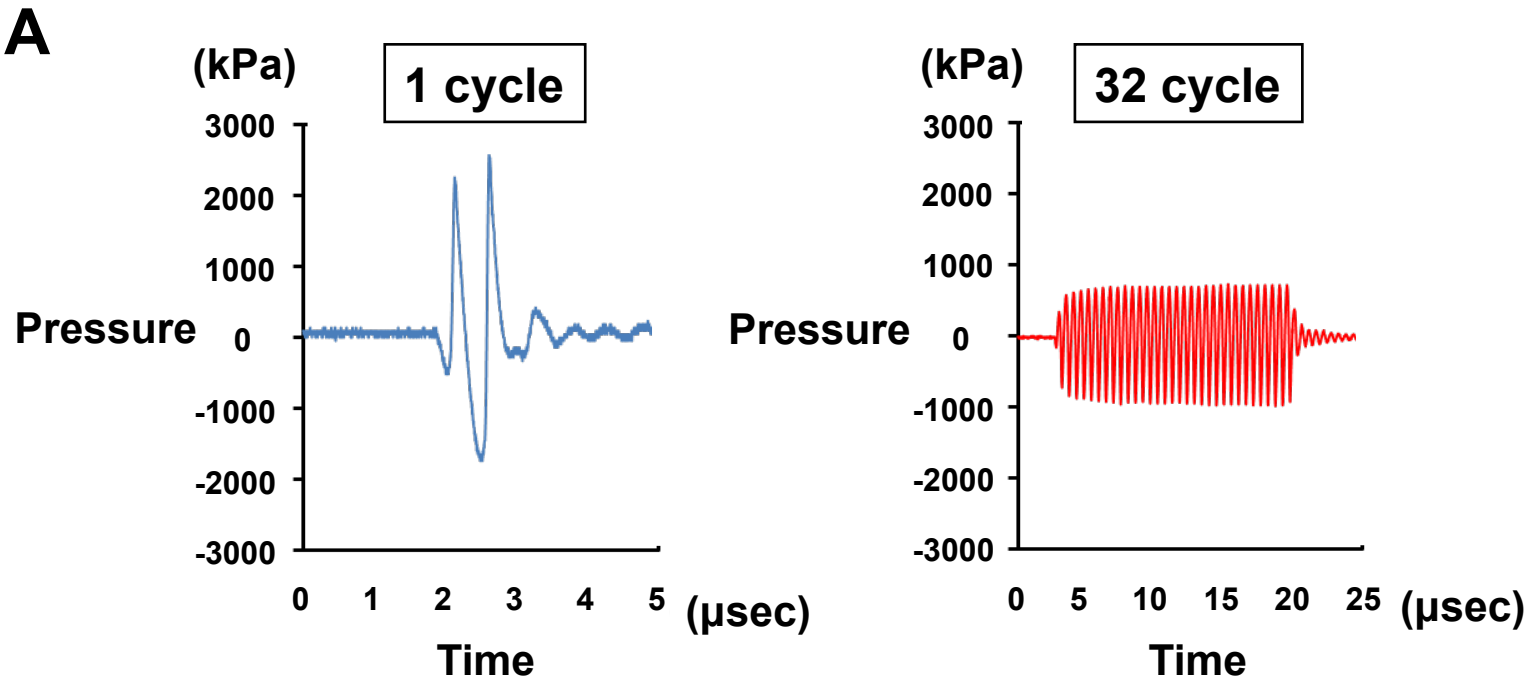

Supplemental Figure I. Effects of the LIPUS Therapy on BW and LV Wall Thickness after AMI in Mice in Vivo
A. Acoustic pressure at 1 and 32 cycles. **B.** Schematic illustration of in vivo study.
C. Body weight (BW) was comparable among the 4 groups. Graph showing the time course of left ventricular anterior wall dimension at end-diastole (LVAWDd), and left ventricular posterior wall dimension at end-diastole (LVPWDd). Results are expressed as mean ± SD.

Supplemental Figure I

B

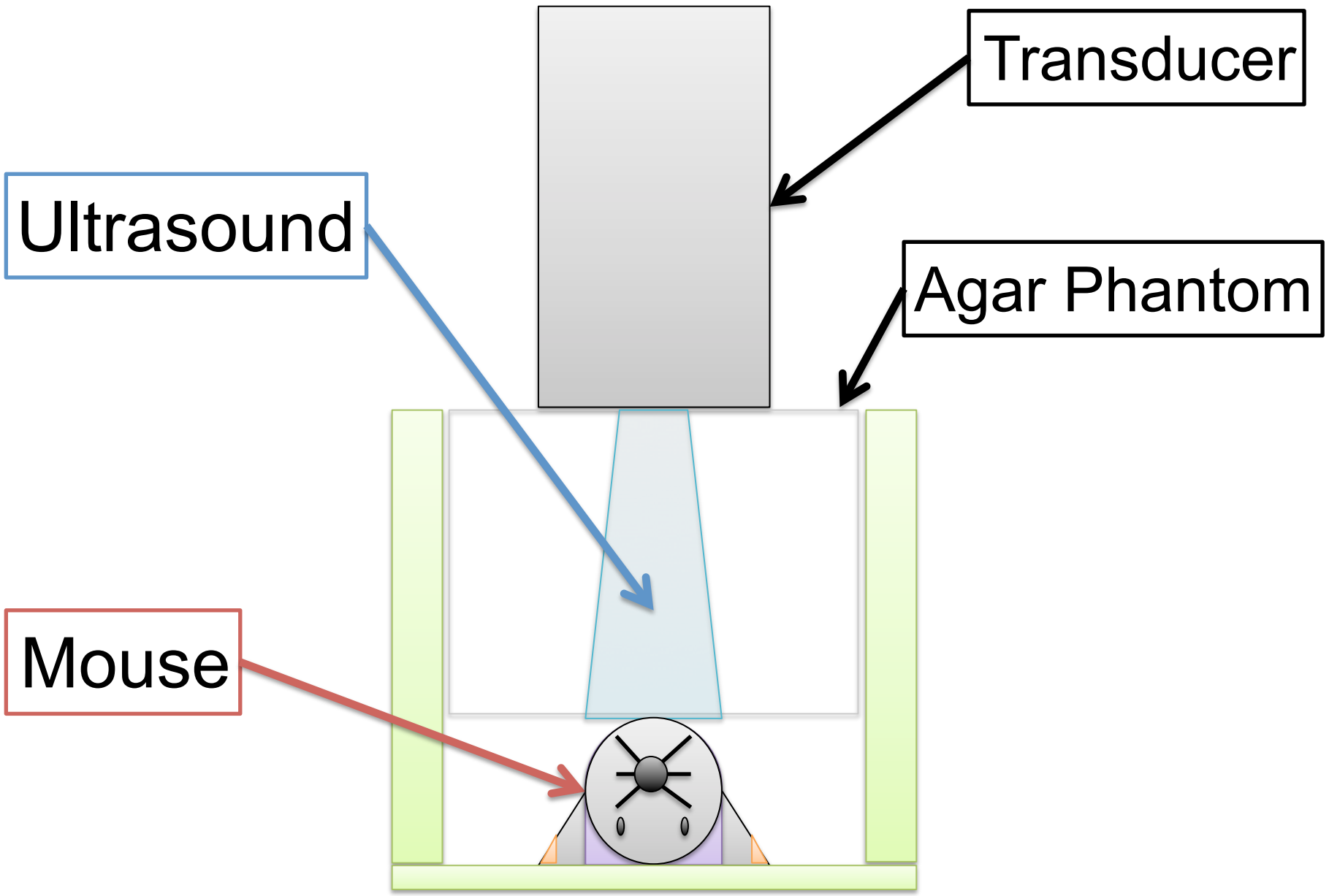

Supplemental Figure I

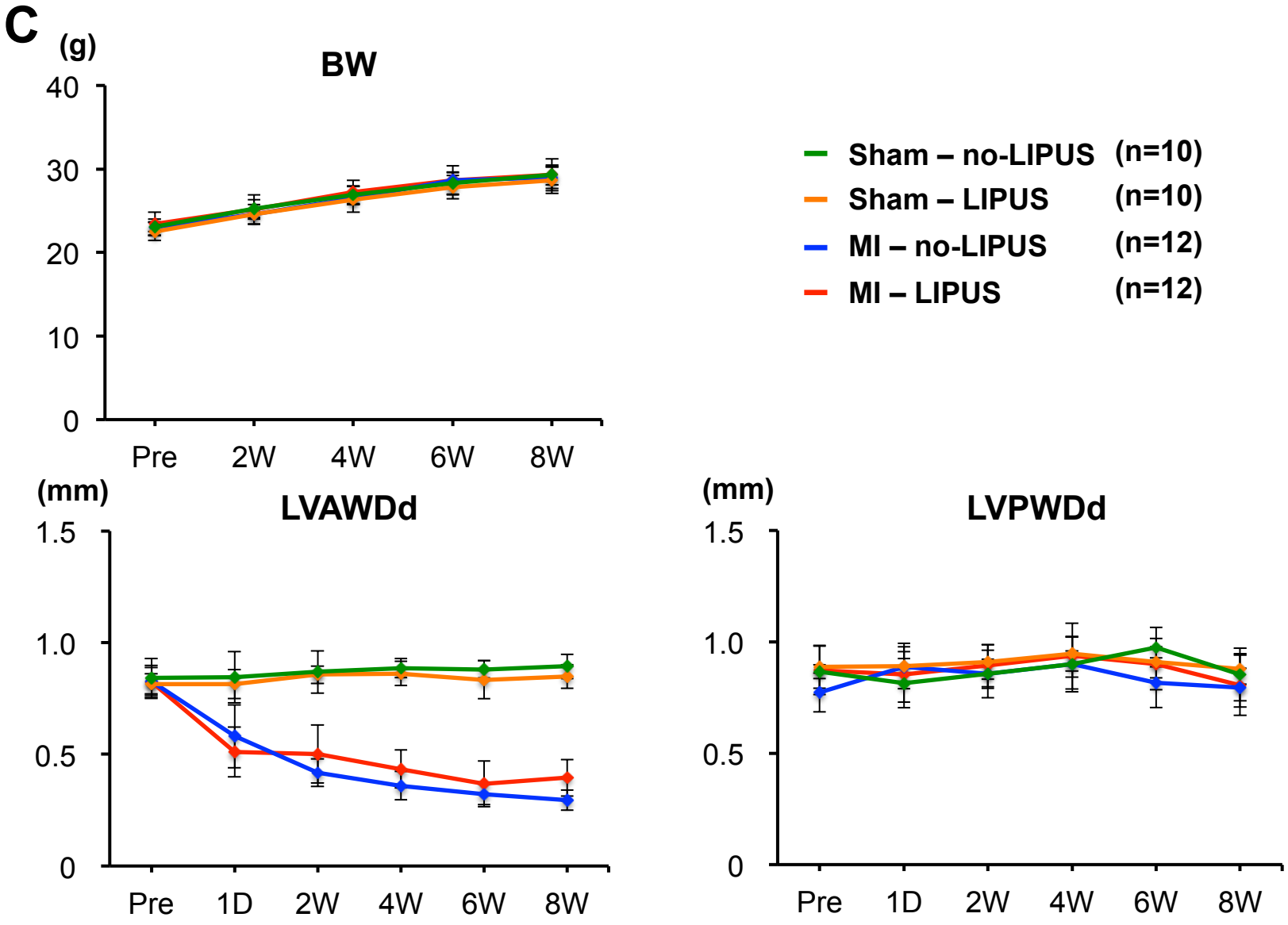

Supplemental Figure II

A

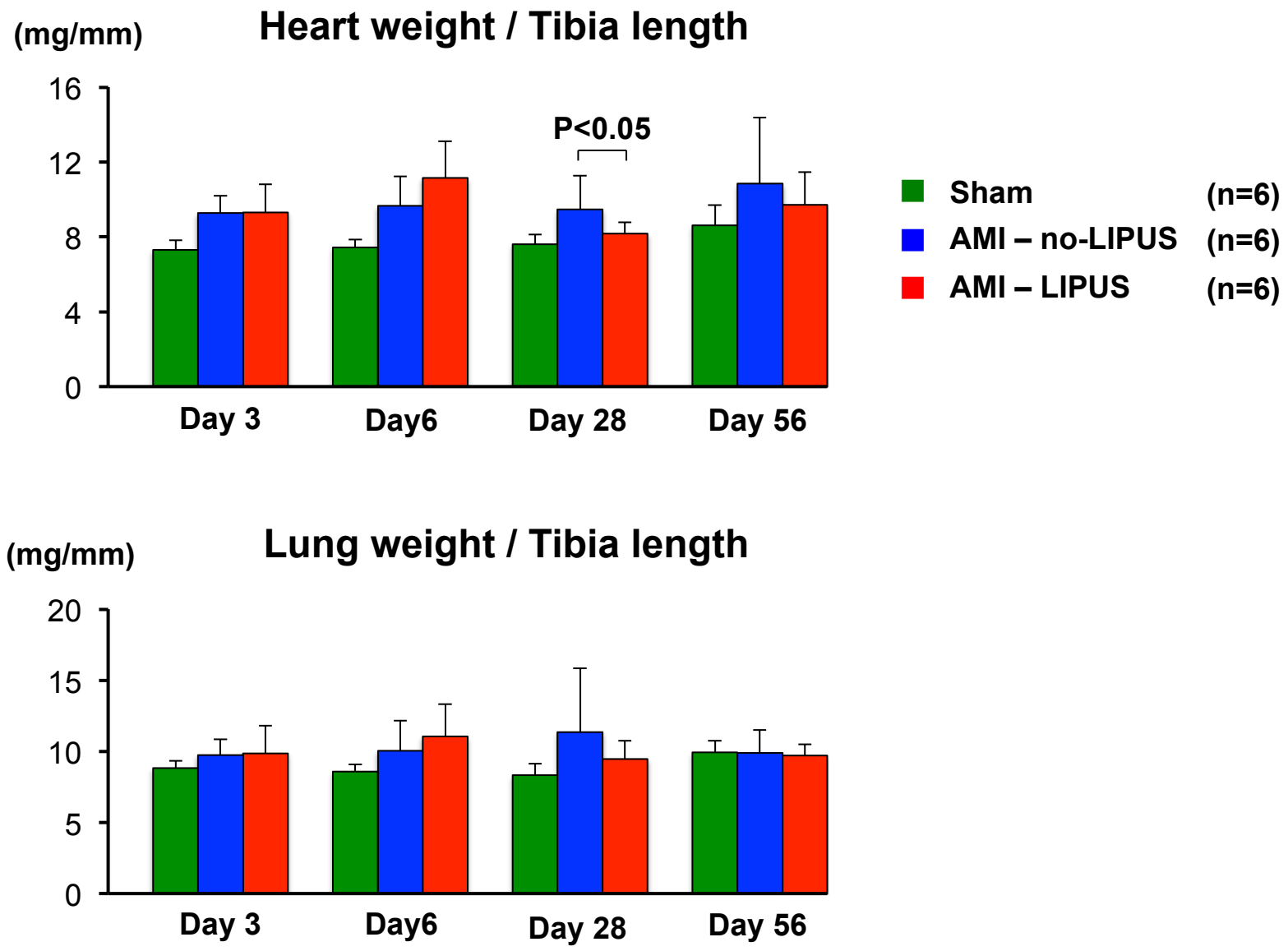

Supplemental Figure II

B

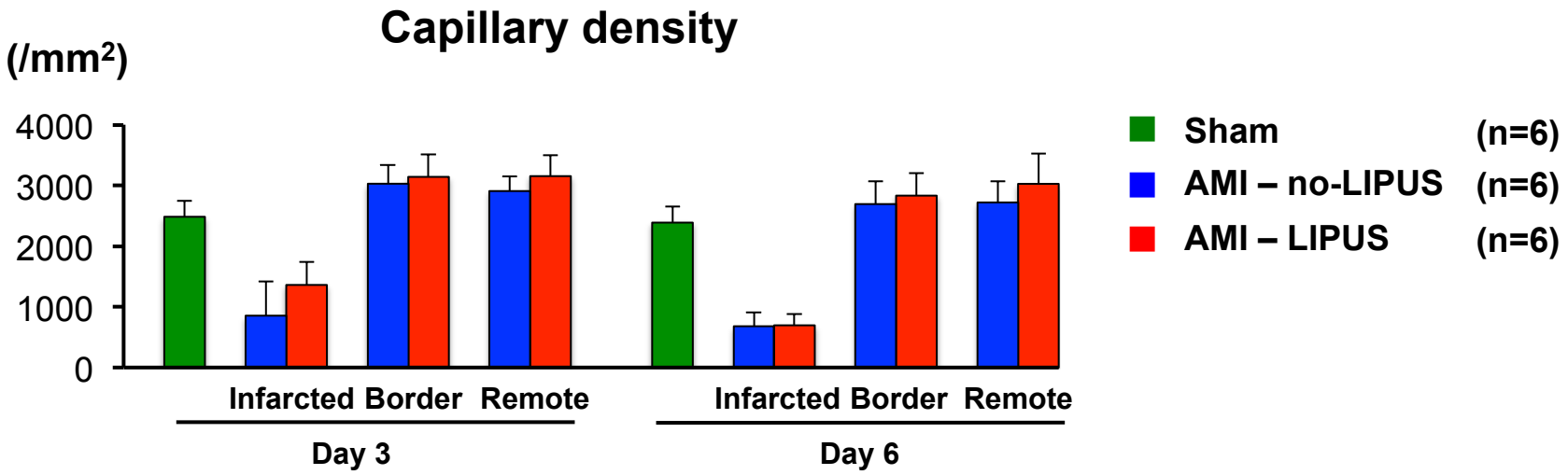

C

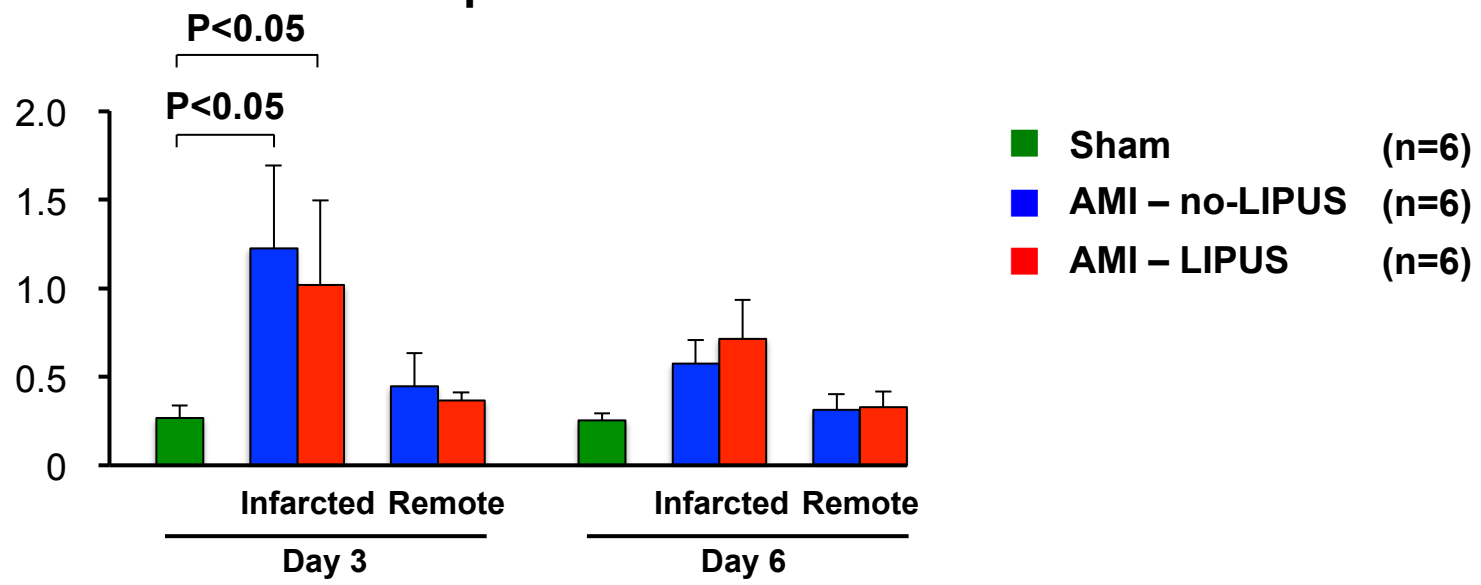

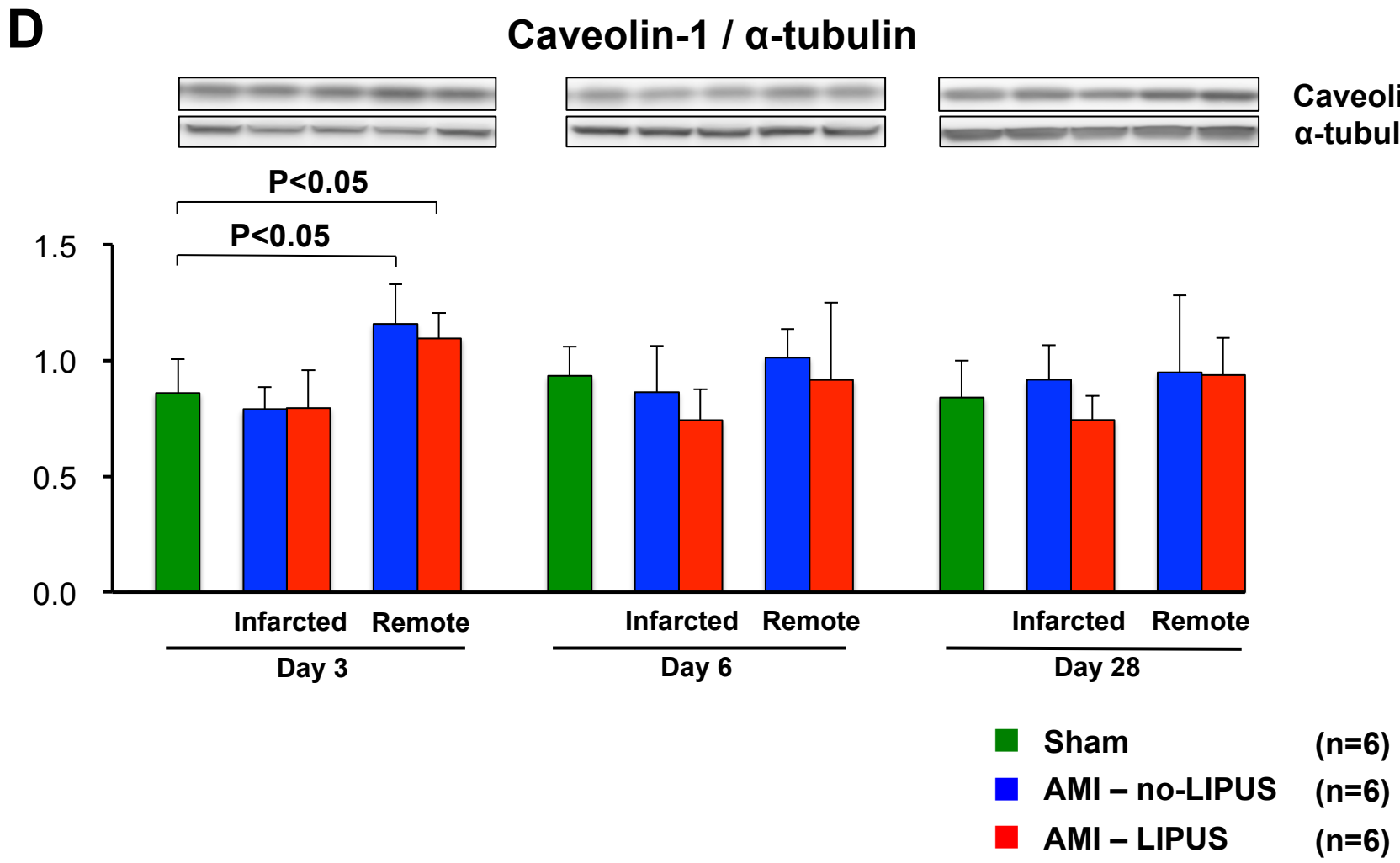

Supplemental Figure II. Effects of the LIPUS Therapy on Histopathological Findings and Molecular Expressions after AMI in Mice

A. The time course of heart weight/tibia length (HW/TL) ratio and lung weight/tibia length (LW/TL) ratio. **B.** Capillary density at 3 and 6 days after AMI. **C.** TGF-β1 mRNA expression at 3 and 6 days after AMI. **D.** Protein levels of caveolin-1. Results are expressed as mean ± SD.

Supplemental Figure III

A

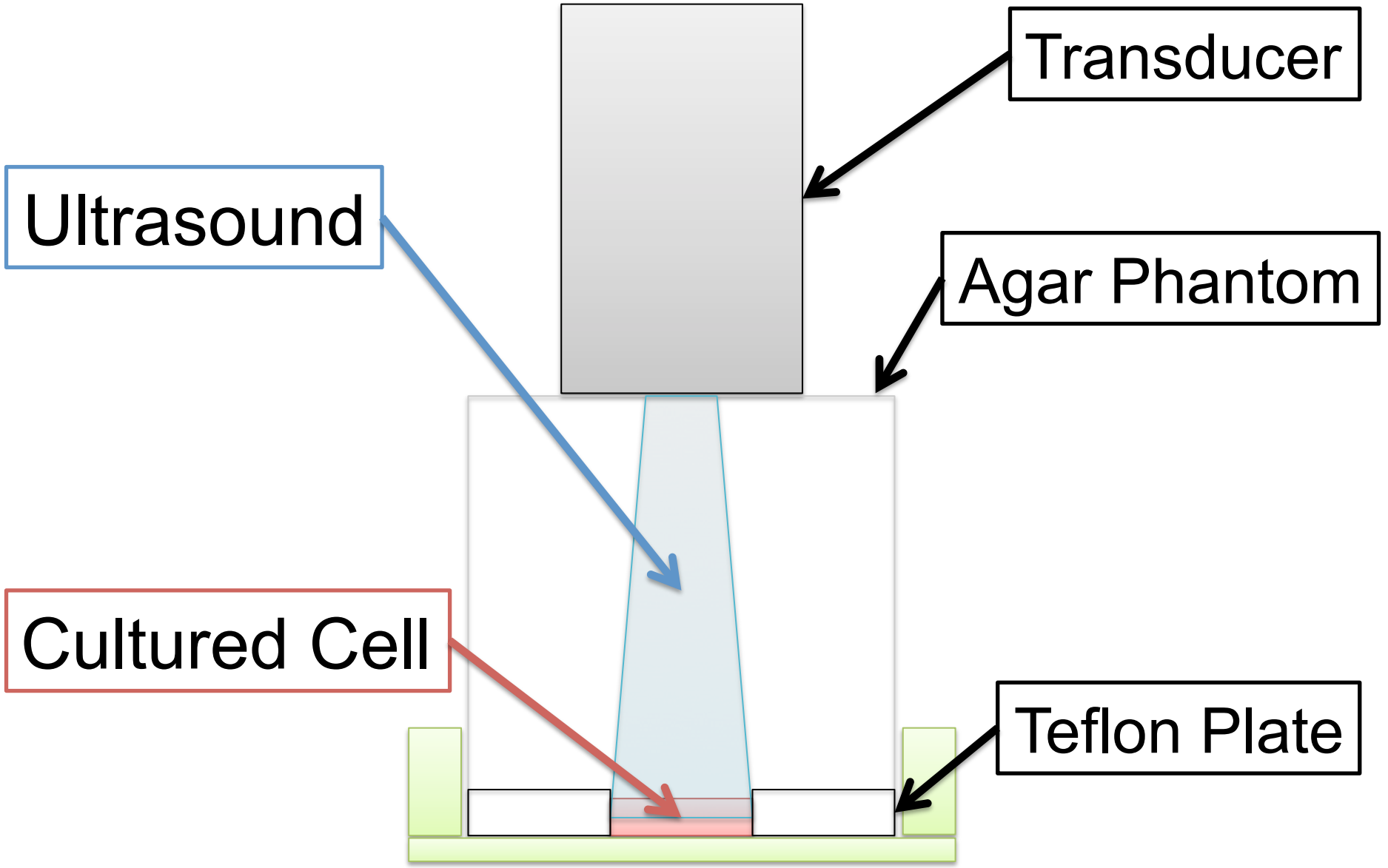

Supplemental Figure III

B

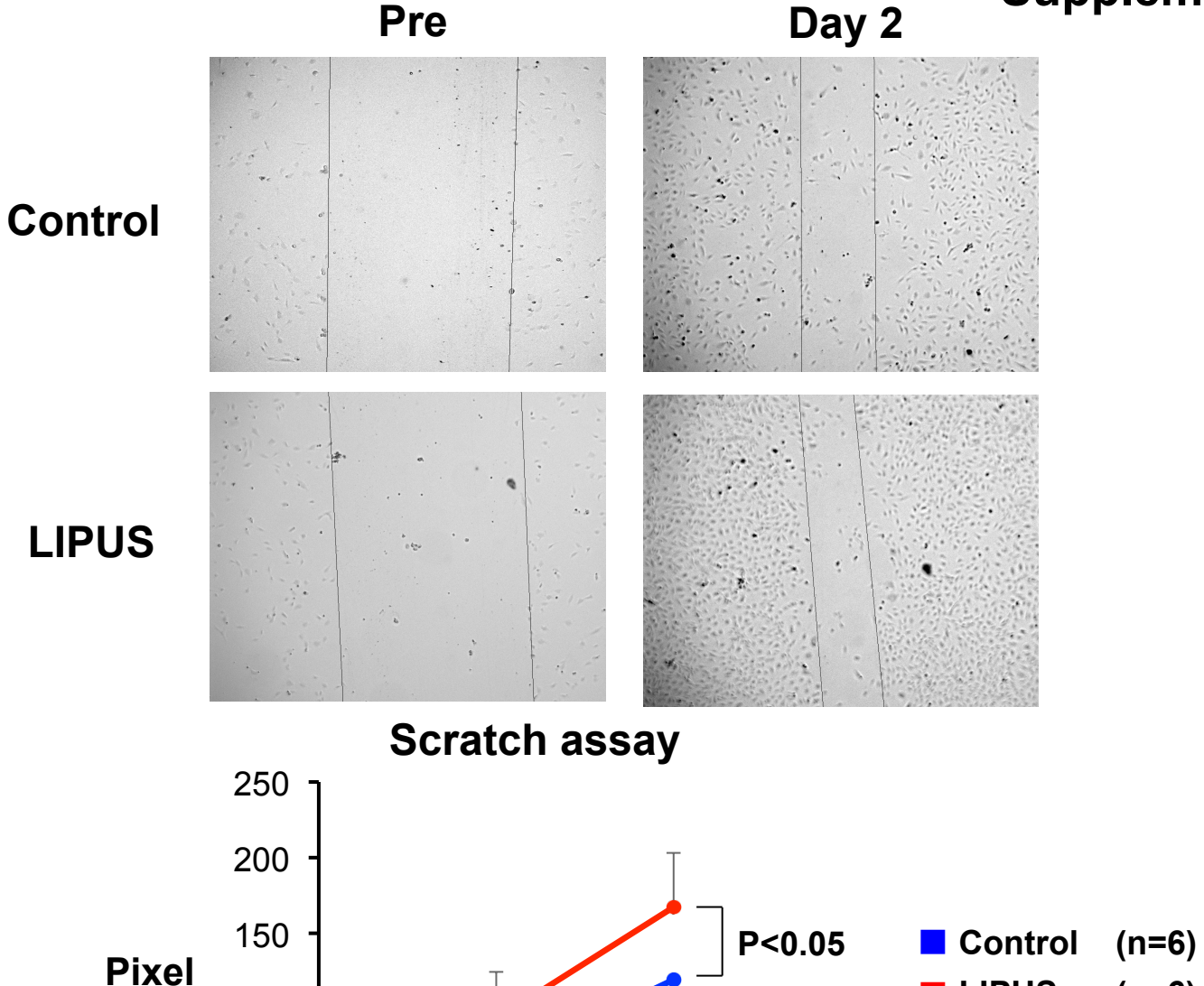

Supplemental Figure III

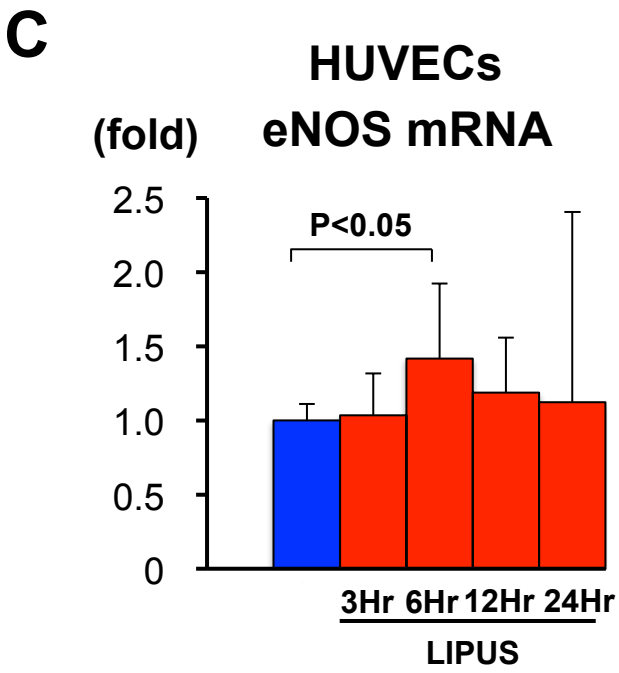

D

Supplemental Figure III

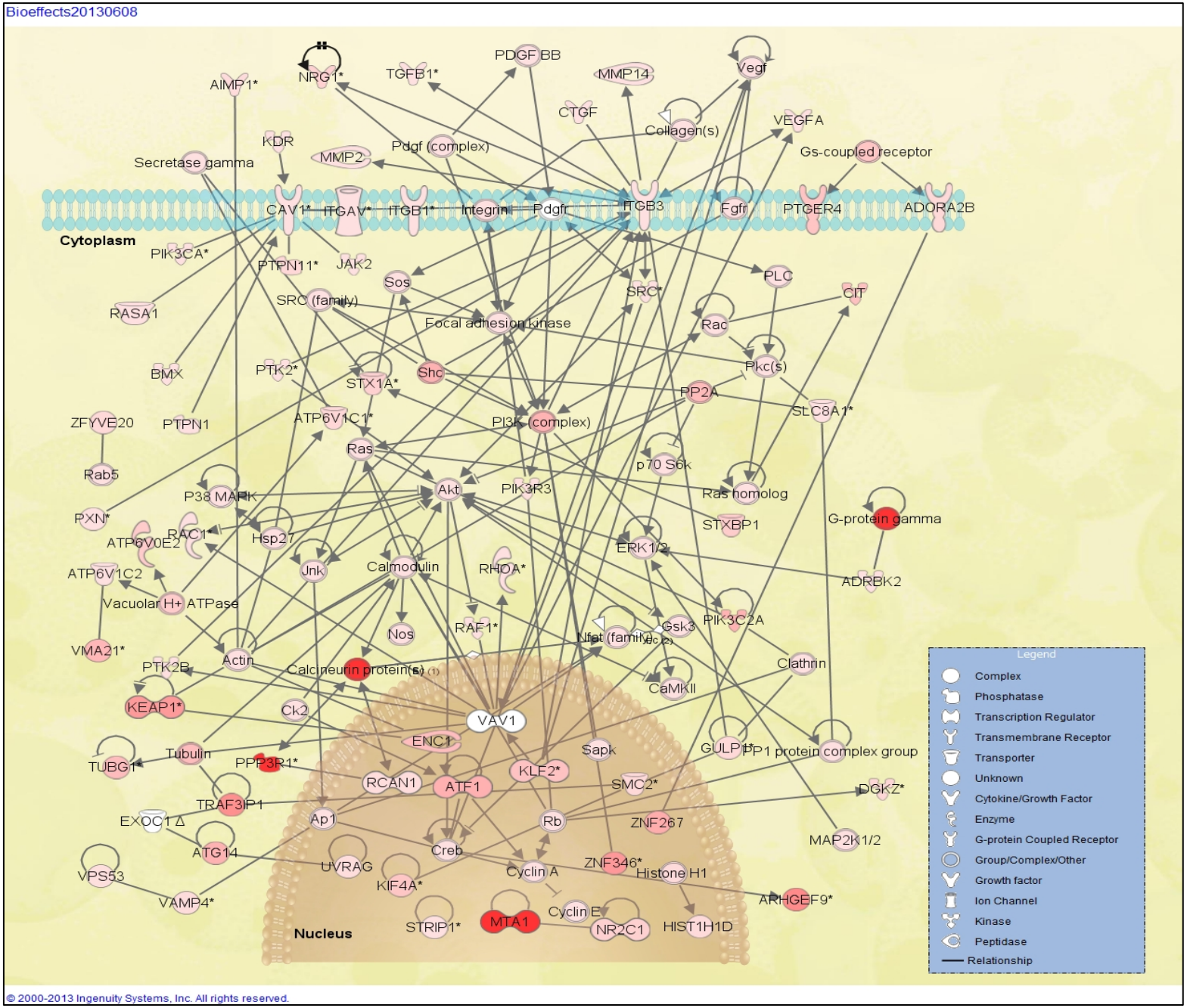

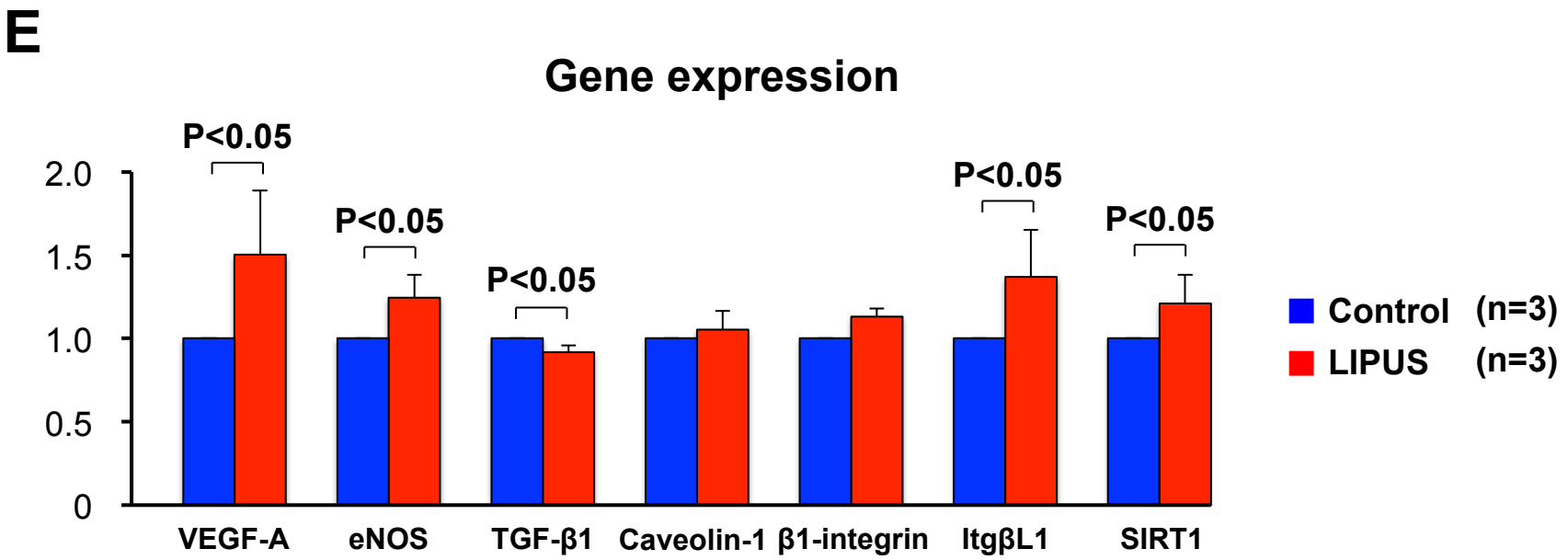

Supplemental Figure III. Effects of the LIPUS on MAPK and PI3K-Akt Signaling
A. Schematic illustration of in vivo study. **B.** The results of scratch assay that shows the effect of LIPUS on proliferation in HUVECs. **C.** mRNA expression of eNOS in HUVECs in response to LIPUS. **D.** To examine gene ontology, including biological processes, cellular components, molecular functions and genetic networks, the obtained microarray data were analyzed using Ingenuity Pathway Analysis tools (Ingenuity Systems, Mountain View, CA, USA), a web-delivered application that enables the identification, visualization and exploration of molecular interaction networks from gene expression data. The schematic illustration represents LIPUS-induced molecular interactions including focal adhesion pathway, MAPK signaling pathway and PI3K-Akt signaling pathway. **E.** The part of expression data of microarray, showing that VEGF-A, eNOS, Integrin β1-like protein, SIRT1 were significantly up-regulated in response to the LIPUS. Results are expressed as mean ± SD.

Supplemental Figure IV

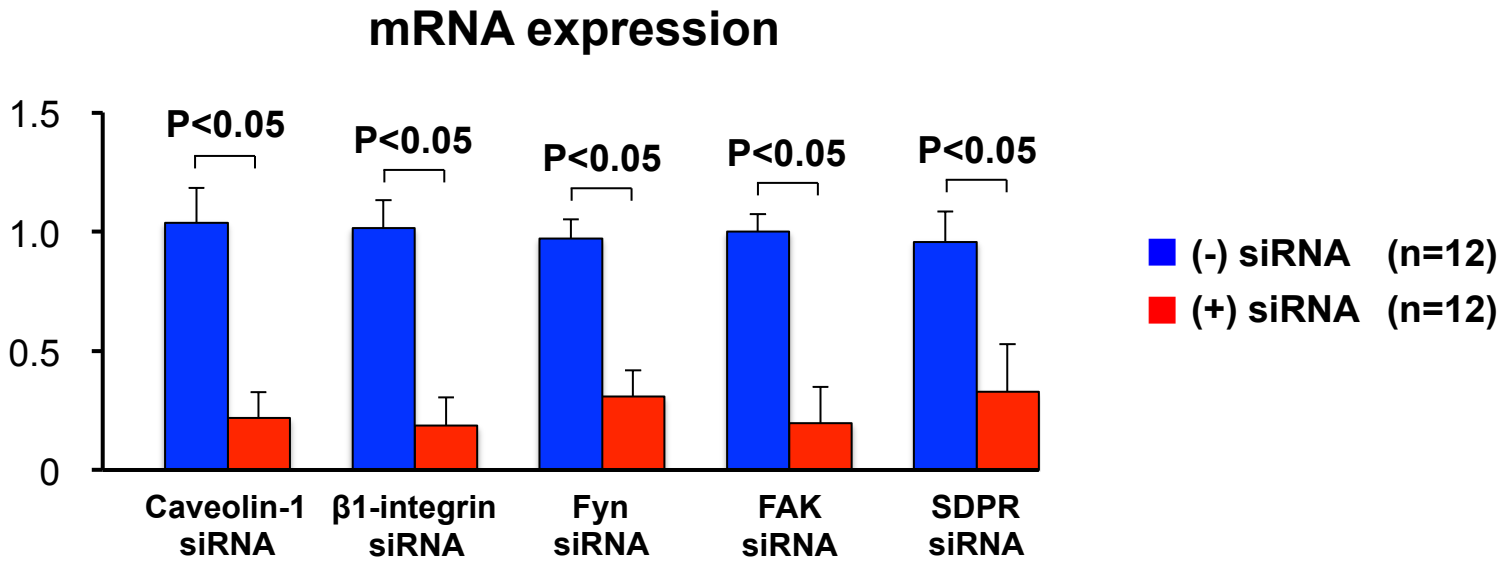

Supplemental Figure IV. Confirmation of Knockdown with siRNA of Each Molecule by Real-time PCR
Knockdown of caveolin-1, β1-integrin, Fyn, FAK and SDPR with siRNA was confirmed. Results are expressed as mean ± SD.

Supplemental Figure V

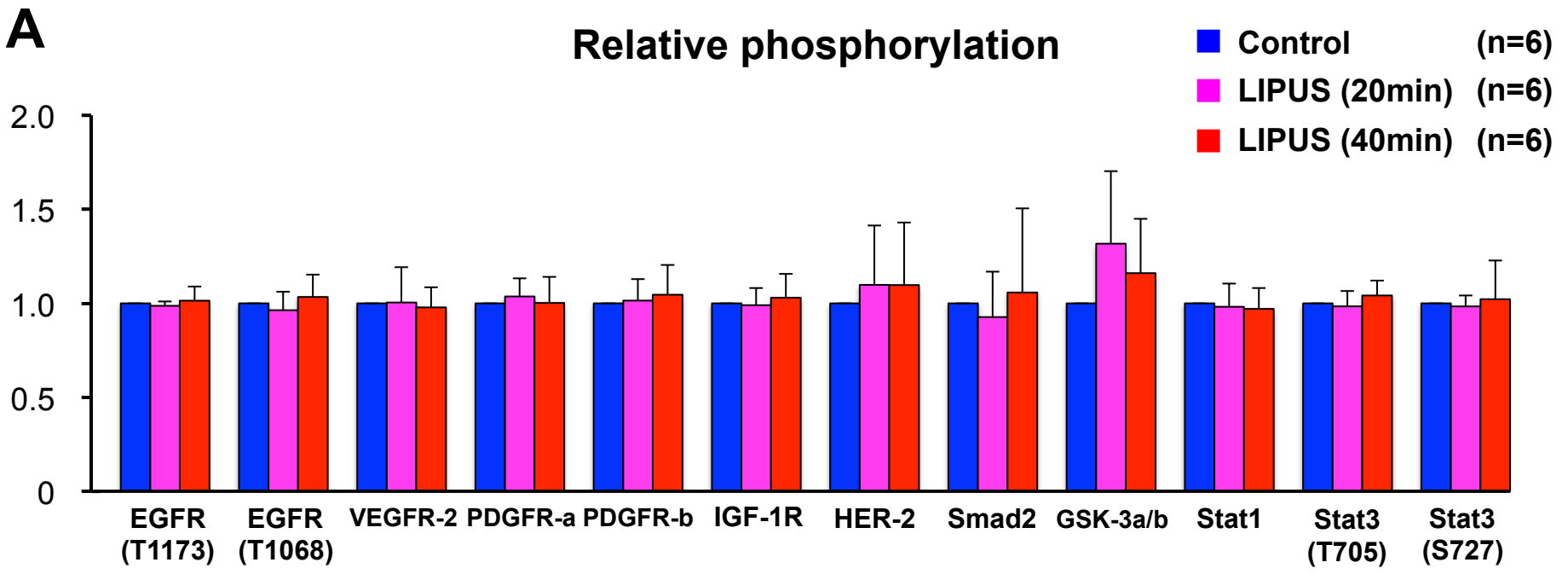

Supplemental Figure V

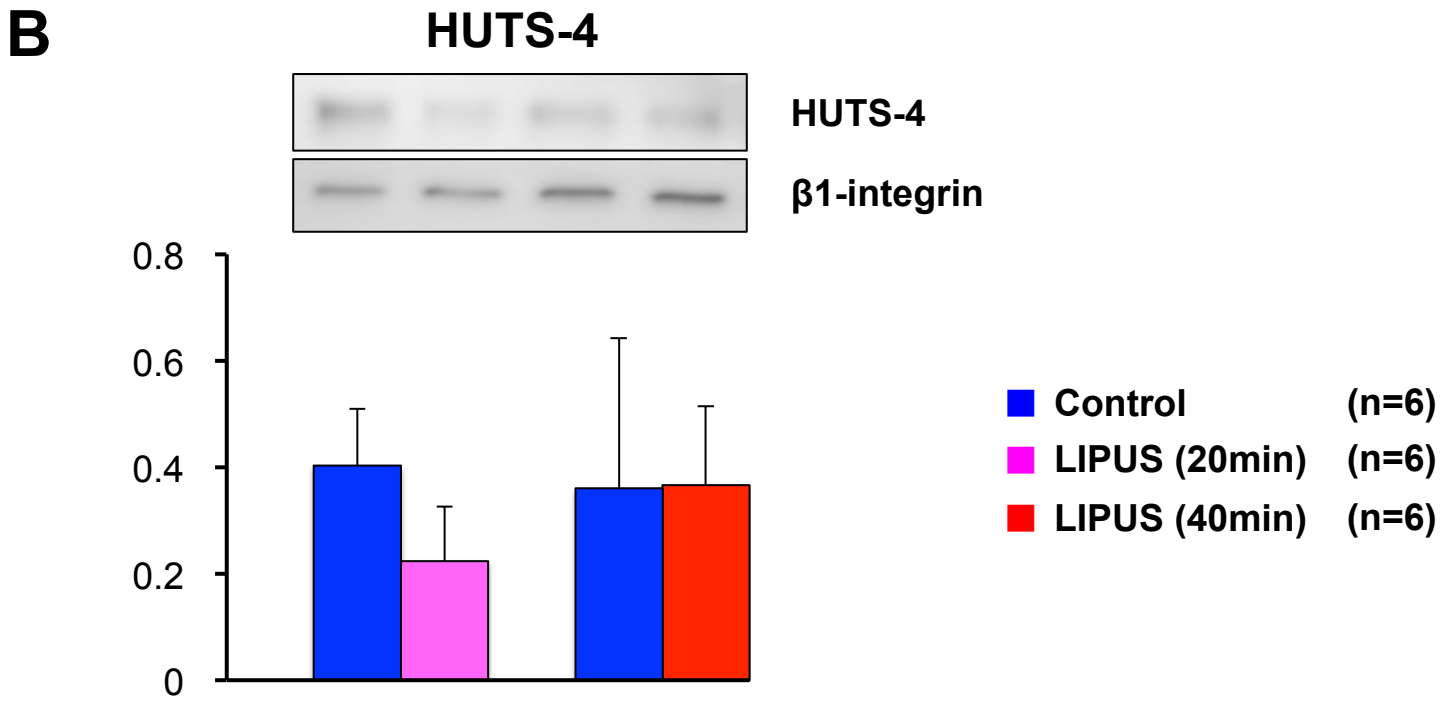

Supplemental Figure V

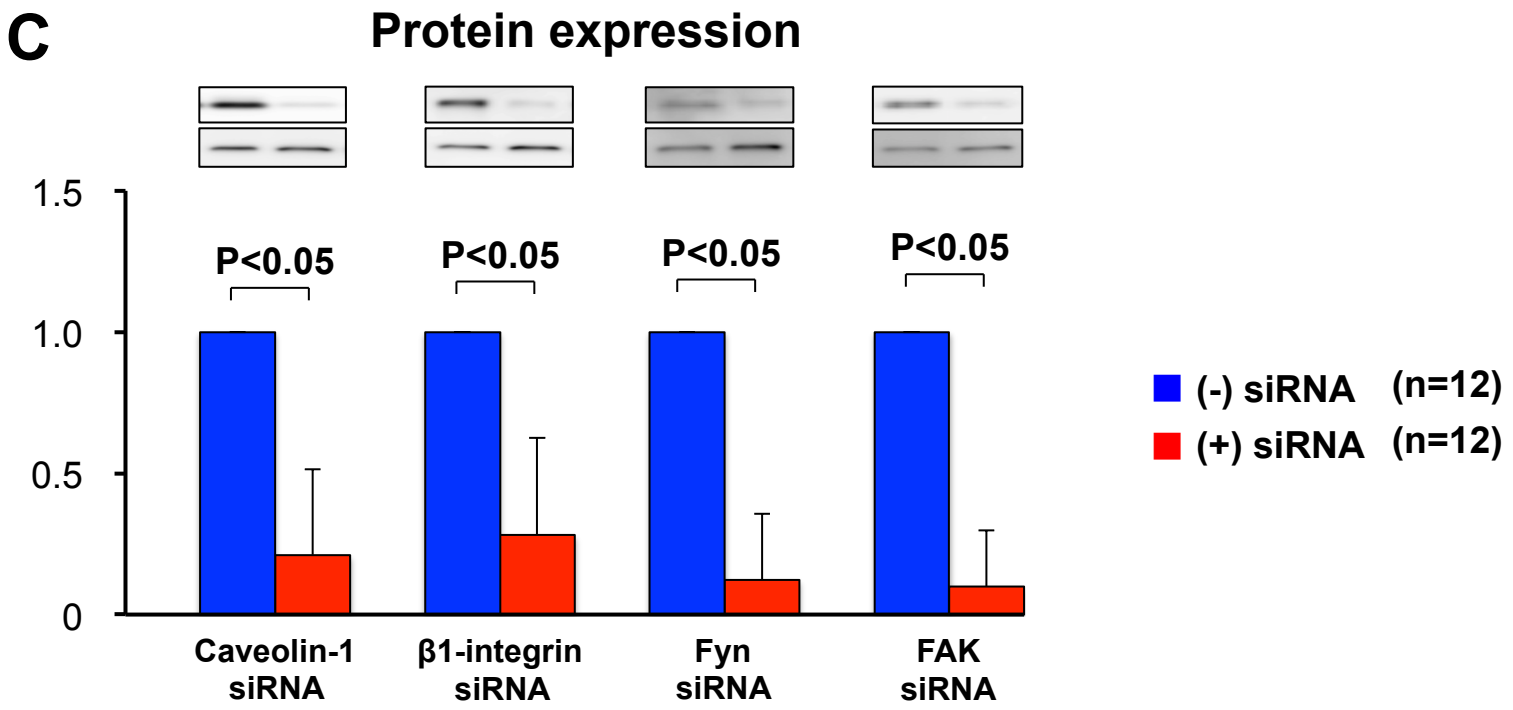

Supplemental Figure V. Bio-Plex Analysis of Phosphorylation of Growth Factors and Second Messengers
A. The results of the phosphoprotein assay with Bio-Plex of LIPUS-irradiated HUVECs at 20 or 40 min are shown. **B.** The results of Western blot analysis of HUTS-4 which related to activation of β1-integrin. **C.** Confirmation of knockdown with siRNA of each molecule by Western blotting. Knockdown with siRNA of caveolin-1, β1-integrin, Fyn, FAK with siRNA was performed. Results are expressed as mean ± SD.

Supplemental Figure VI

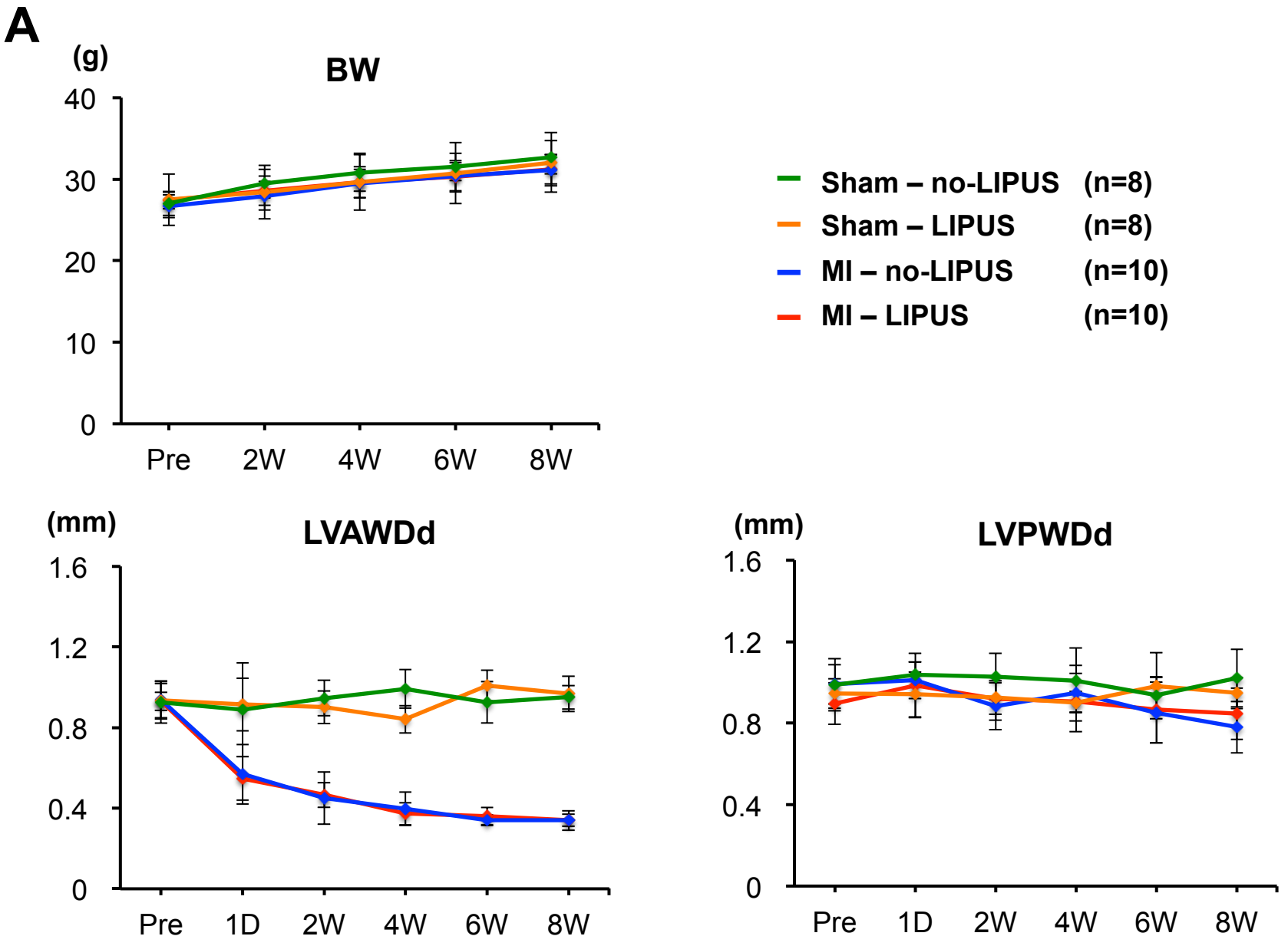

Supplemental Figure VI

B

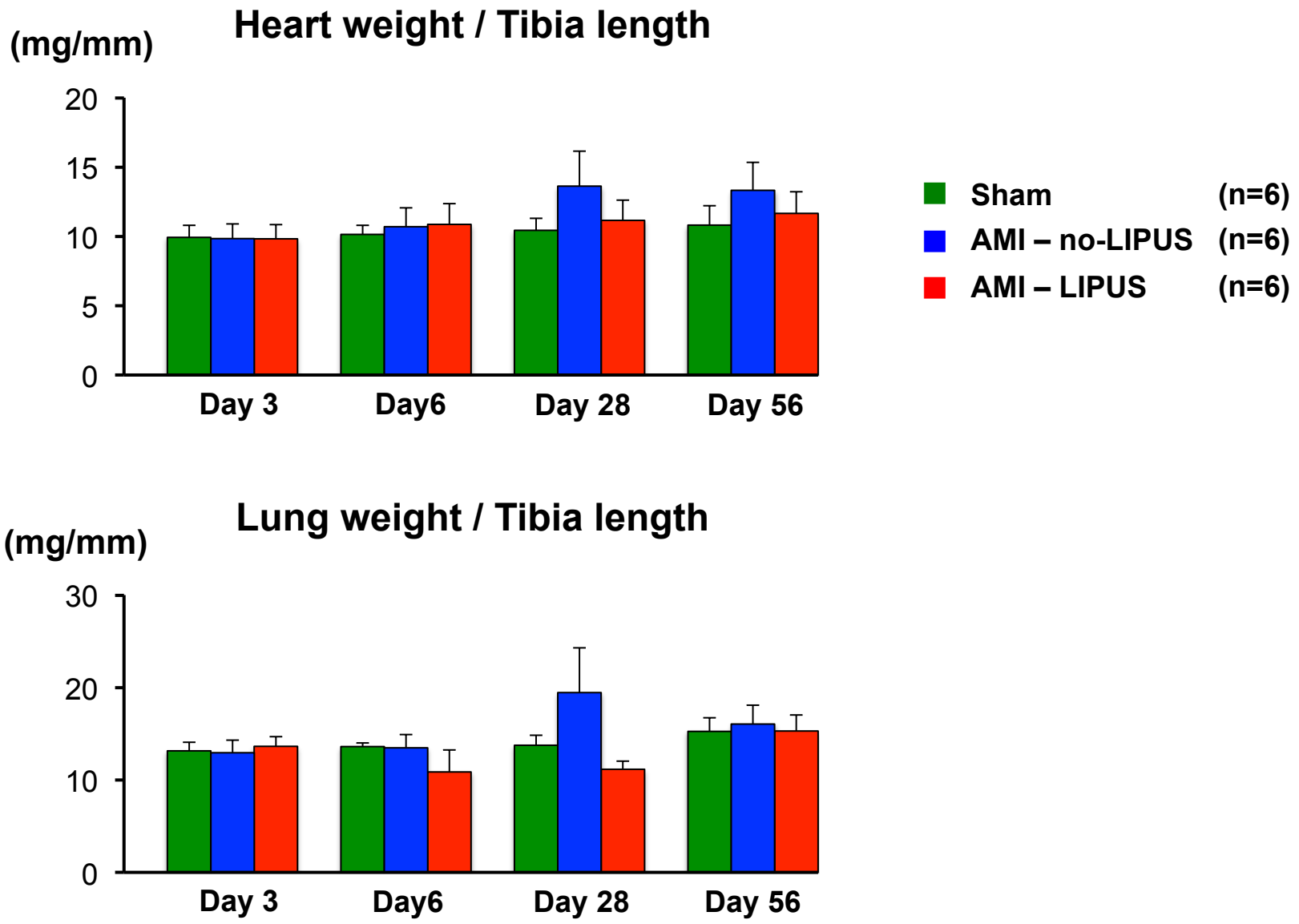

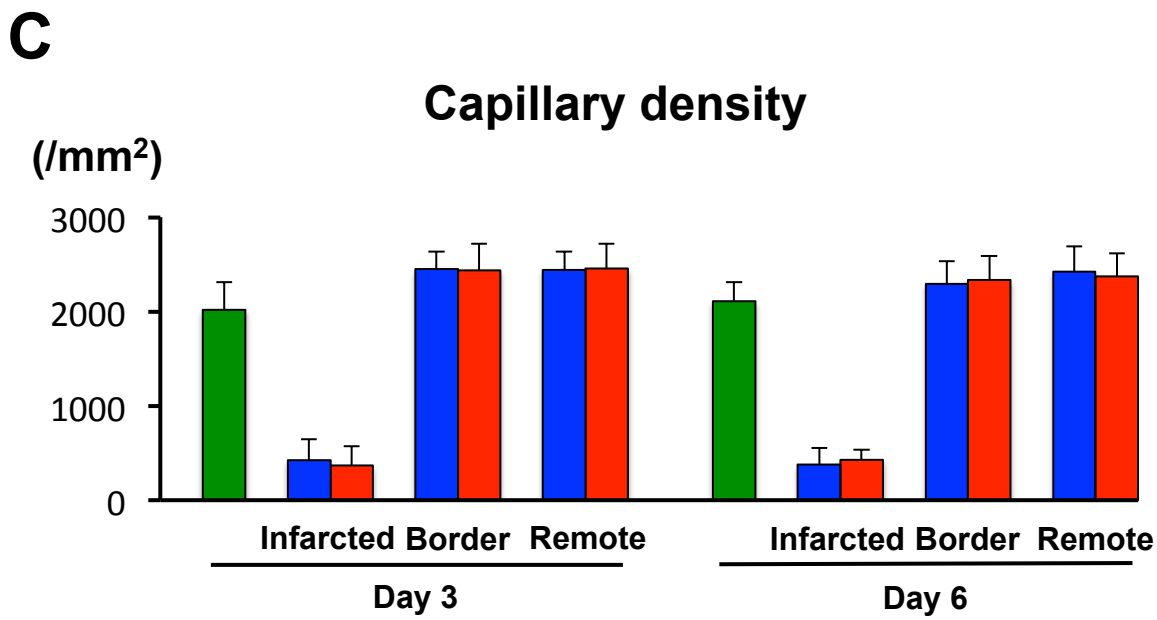

Supplemental Figure VI. Effects of the LIPUS Therapy on BW, LV Wall Thickness, and Histopathological Findings after AMI in Cav-1-KO Mice in Vivo

A. Graphs showing the time course of the BW, left ventricular anterior wall dimension at end-diastole (LVAWDd), left ventricular posterior wall dimension at end-diastole (LVPWDd). **B.** The time course of heart weight/tibia length (HW/TL) ratio and lung weight/tibia length (LW/TL) ratio. **C.** Capillary density at 3 and 6 days after MI in each zone. Results are expressed as mean ± SD.

Supplemental Figure VII

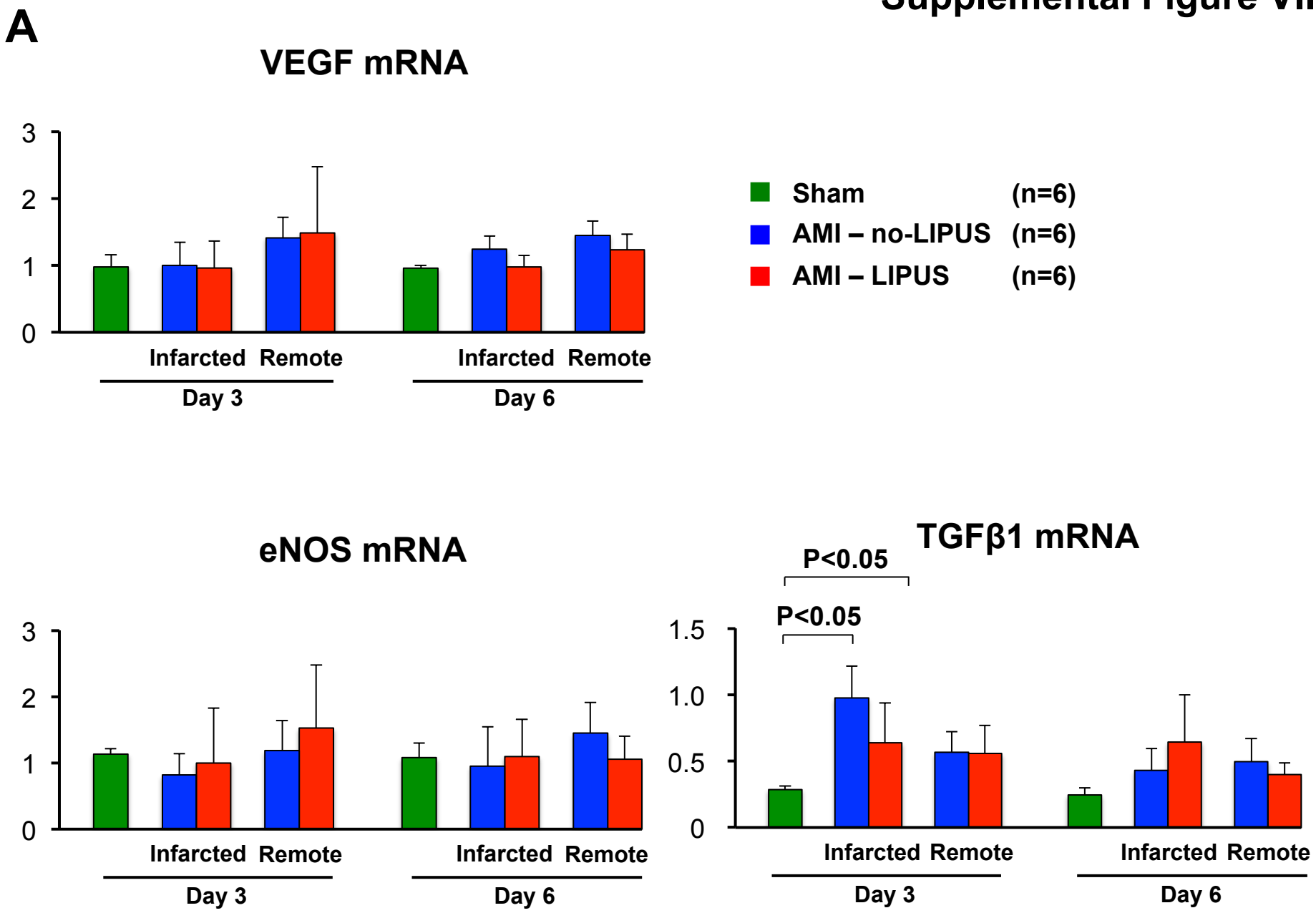

B

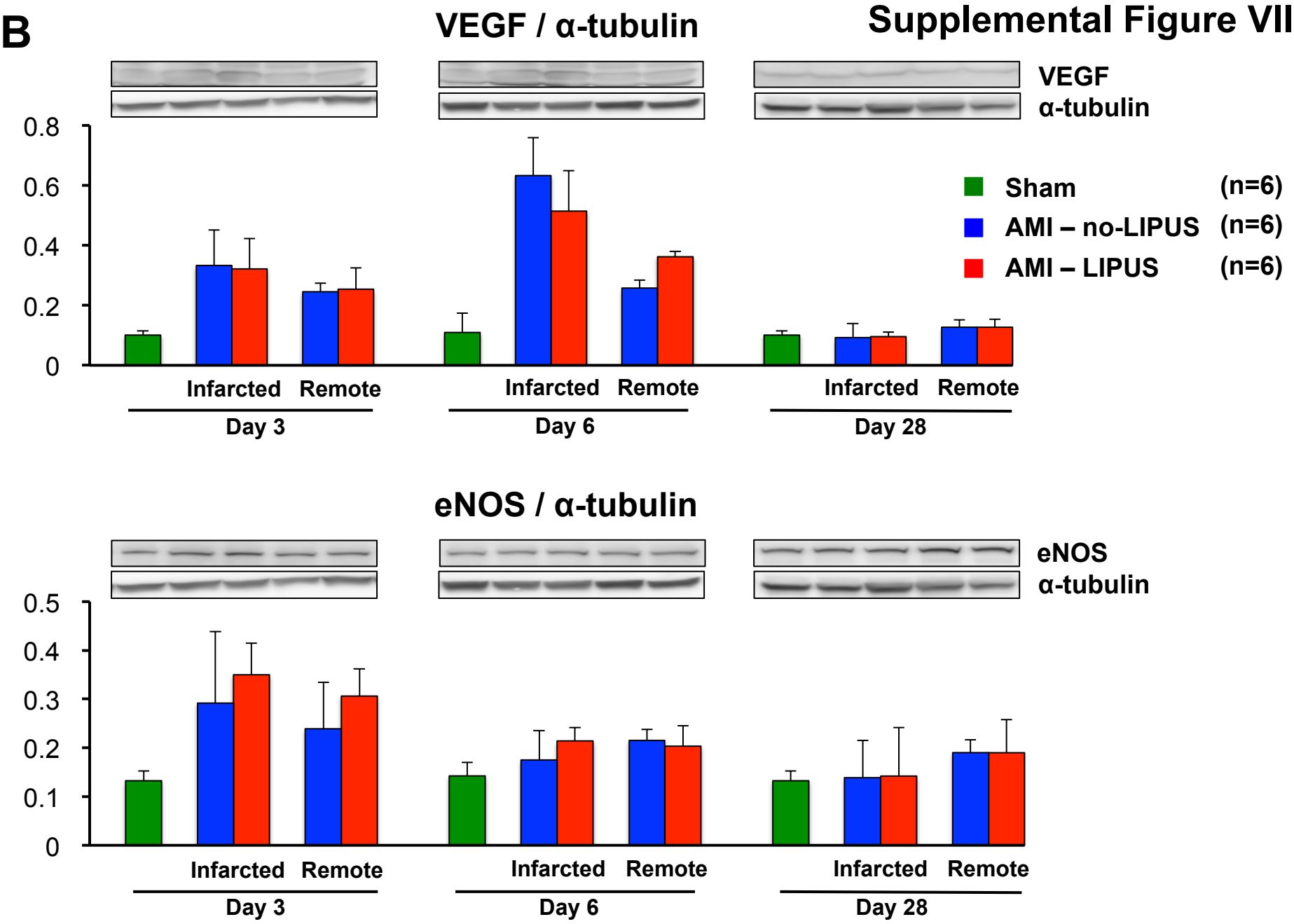
VEGF / α-tubulin
VEGF
α-tubulin
0.8
0.6
0.4
0.2
0
Sham (n=6)
AMI – no-LIPUS (n=6)
AMI – LIPUS (n=6)
Infarcted
Remote
Day 3
Day 6
Day 28
eNOS / α-tubulin
eNOS
α-tubulin
0.5
0.4
0.3
0.2
0.1
0

Supplemental Figure VII

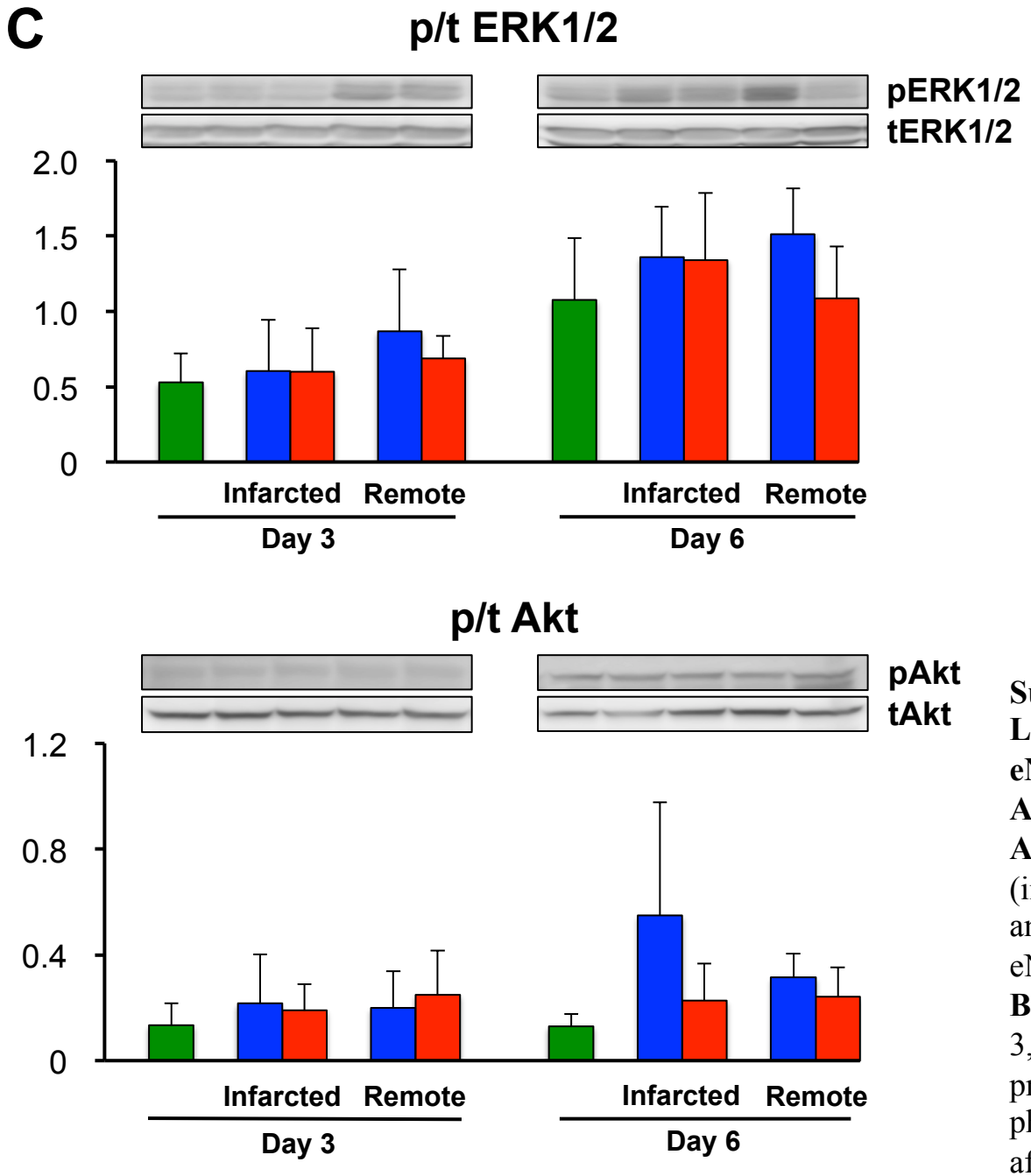

Supplemental Figure VII. No Effects of the LIPUS Therapy on Expression of VEGF and eNOS and Phosphorylation of ERK1/2 and Akt in Cav-1-KO Mice in Vivo

A. Left ventricular lysates from infarcted (includes border) and remote regions were analyzed for mRNA expression of VEGF, eNOS and TGFβ1 at 3 and 6 days after AMI. **B-C.** Western blot analysis was performed at 3, 6 and 28 days after AMI to determine the protein expression of VEGF, eNOS, and phosphorylation of ERK1/2 (**C**) and Akt (**C**) after MI. Results are expressed as mean ± SD.

Supplemental Figure VIII

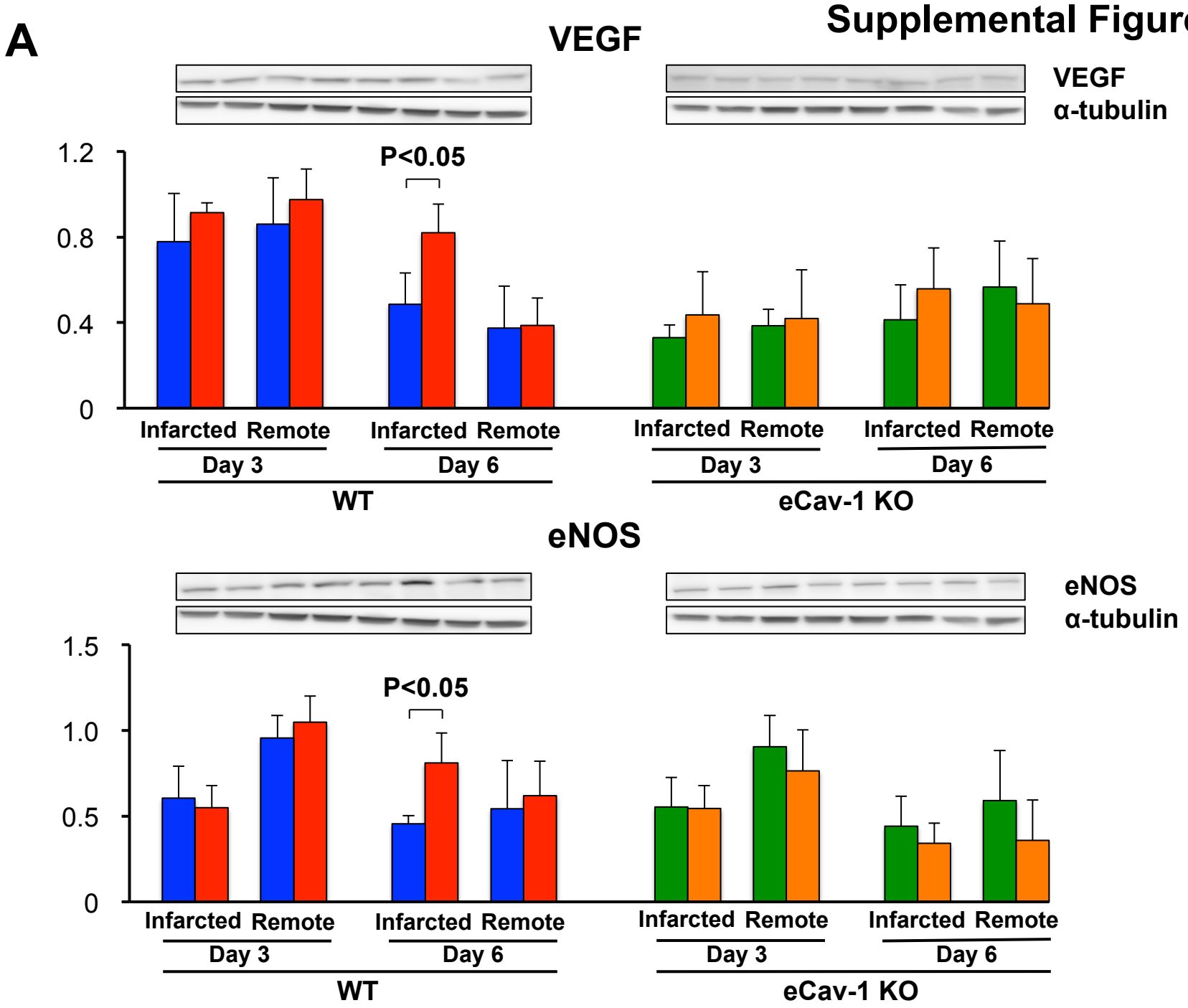

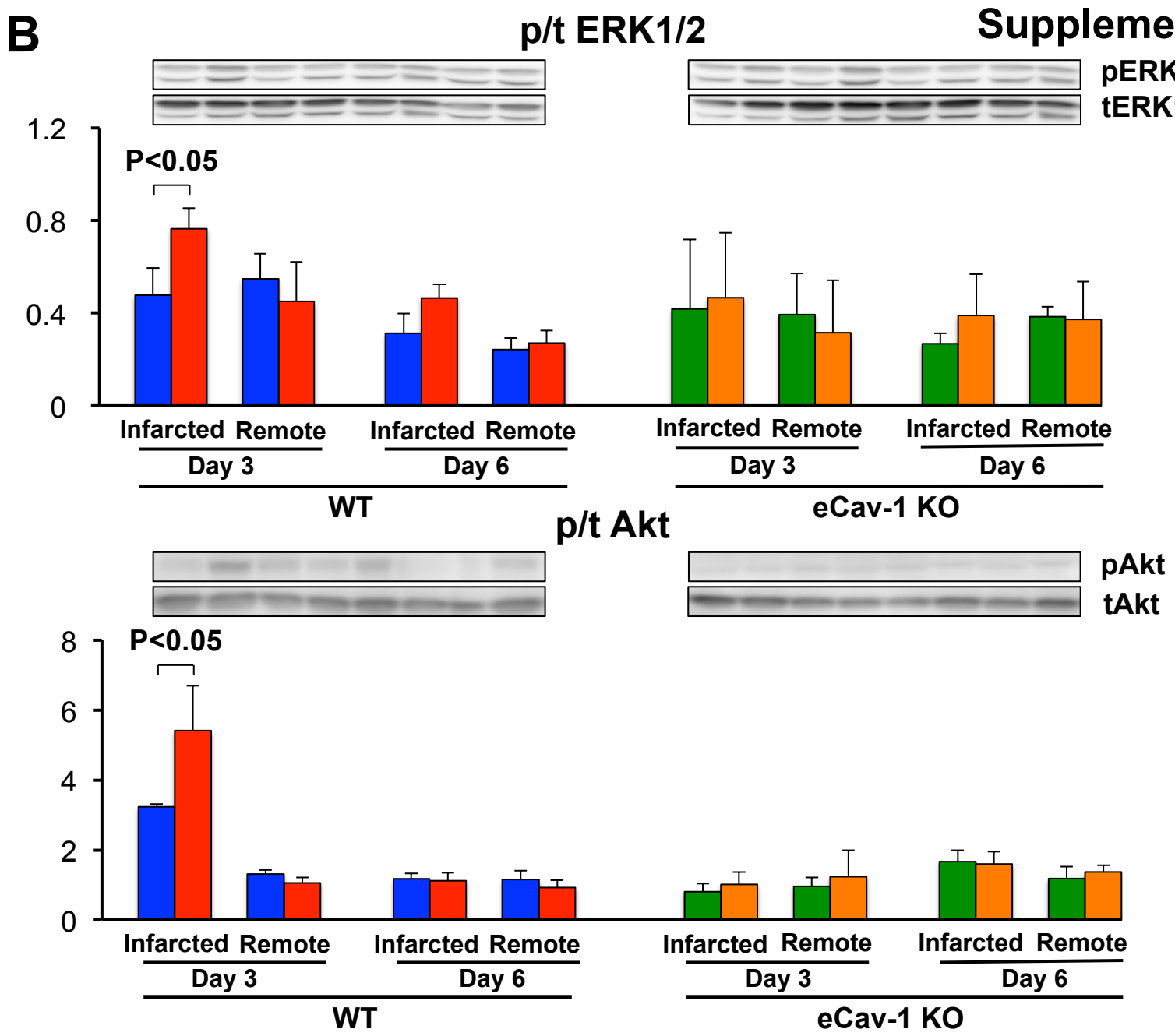

Supplemental Figure VIII. LIPUS-induced up-regulation of angiogenic molecules were also blunted in eCav-1-KO mice
A. Protein levels of VEGF and eNOS. **B.** Phosphorylation of ERK1/2 and Akt. Results are expressed as mean ± SD.

Supplemental Figure IX

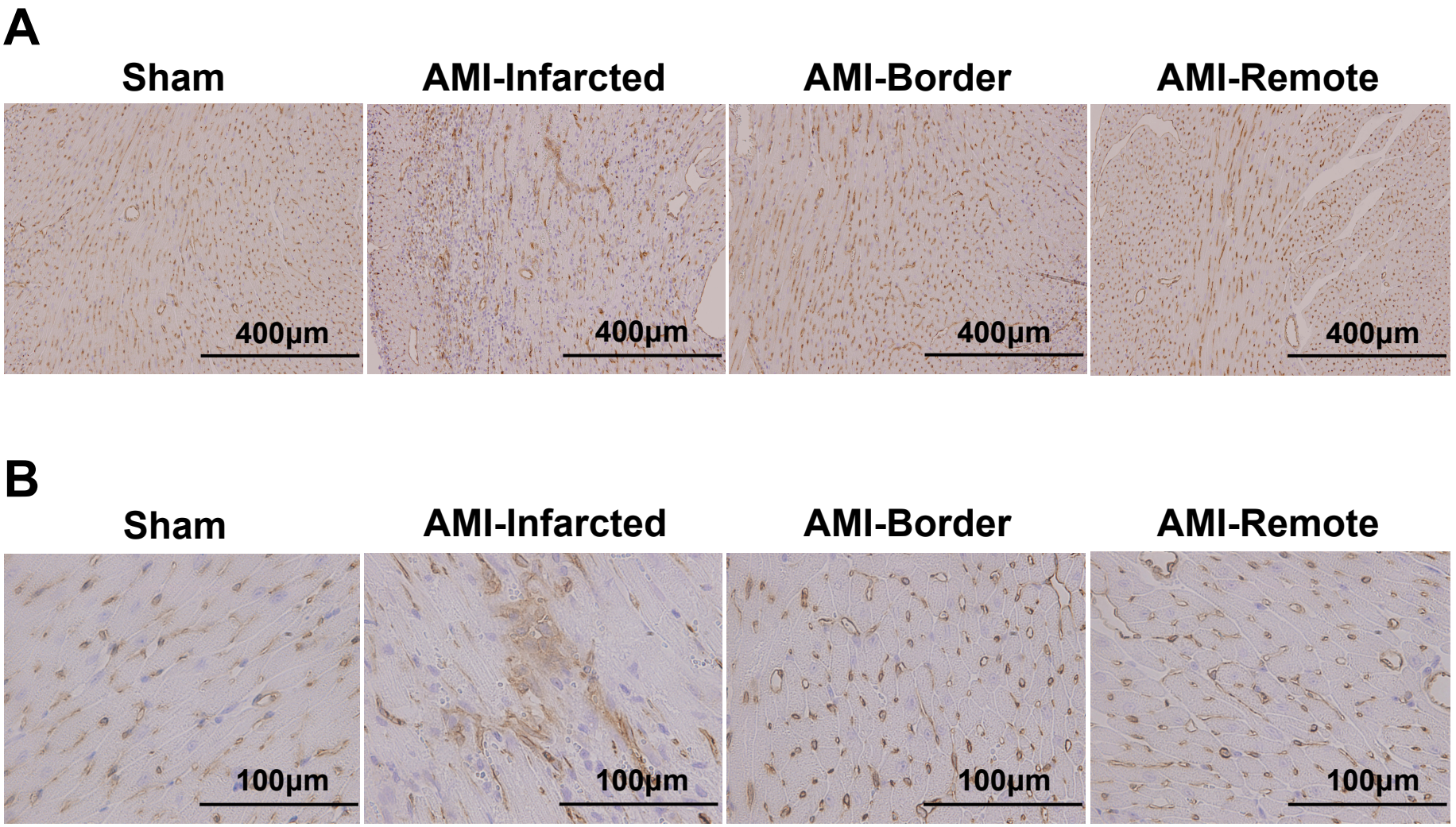

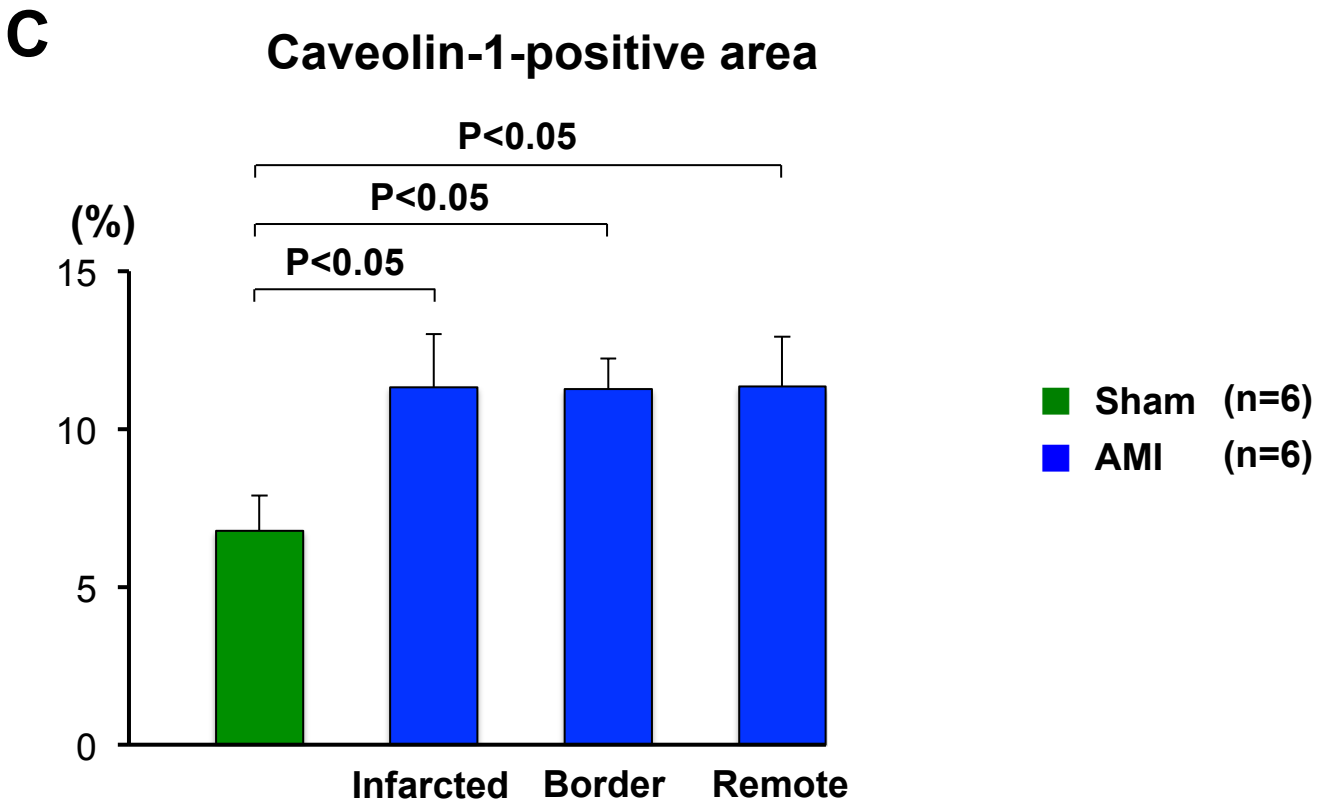

Supplemental Figure IX. Rapid response of caveolin-1 expression was found in histological examination after MI in vivo.

A. Representative photomicrographs of the immunostaining for caveolin-1 in the site of infarcted, border and remote area of WT mice 3 days after AMI. **B.** High-power field of the images shown in A. **C.** %area of the caveolin-1-positive cells analyzed by ImageJ Software (NIH).
Results are expressed as mean ± SD.

Low-intensity Pulsed Ultrasound Enhances Angiogenesis and Ameliorates Left Ventricular Dysfunction in a Mouse Model of Acute Myocardial Infarction

Tomohiko Shindo,[1] Kenta Ito,[1] Tsuyoshi Ogata, [1] Kazuaki Hatanaka,[1] Ryo Kurosawa,[1] Kumiko Eguchi,[1] Yuta Kagaya,[1] Kenichiro Hanawa,[1] Kentaro Aizawa,[1] Takashi Shiroto,[1] Sachie Kasukabe,[1] Satoshi Miyata,[1] Hirofumi Taki,[2,3] Hideyuki Hasegawa,[2,3] Hiroshi Kanai,[2,3] Hiroaki Shimokawa.[1]

[1]Department of Cardiovascular Medicine, Tohoku University Graduate School of Medicine, Sendai, Japan, [2]Department of Electronic Engineering, Graduate School of Engineering, Tohoku University, Sendai, Japan, and [3]Division of Biomedical Measurements and Diagnostics, Graduate School of Biomedical Engineering, Tohoku University, Sendai, Japan.

Running title: LIPUS Ameliorates LV Dysfunction after AMI

Key words: angiogenesis, mechanotransduction, cell signaling, contractile reserve, infarct remodeling

Subject Codes: [27] Other Treatment, [105] Contractile function, [129] Angiogenesis, [138] Cell signaling/signal transduction, [151] Ischemic biology - basic studies.

TOC category: Basic study

TOC subcategory: Vascular Biology

Address for Correspondence:

Kenta Ito, MD, PhD.
Associate Professor
Department of Cardiovascular Medicine
Tohoku University Graduate School of Medicine
1-1 Seiryo-machi, Aoba-ku, Sendai 980-8574, Japan
TEL: +81-22-717-7153, FAX: +81-22-717-7156
E-mail: ito-kenta@cardio.med.tohoku.ac.jp

Materials and Methods

The present study confirms to the Guide for the Care and Use of Laboratory Animals published by the US National Institutes of Health and was performed according to the protocols approved by the Institutional Committee for Use and Care of Laboratory Animals of Tohoku University (2013Ikumikae-135, 2013Idou-516) and the Ethics Committee of Tohoku University Graduate School of Medicine (2014-1-048). Detailed methods are described in the supplemental data.

Animal Models

Male C57BL/6 wild-type (WT) mouse (8-week-old, 20-30g in body weight), caveolin-1-deficient (Cav-1-KO) mice (8-week-old, 22-30g in body weight) and endothelial cell specific caveolin-1-deficient (eCav-1-KO) mice were used in the present study. Cav-1-KO mice were developed by breeding pairs of heterozygous mice (Jackson Laboratory, Barharbor, ME, USA) and were maintained in our institute.[1] The Cav-1-KO mice were backcrossed to C57BL/6 mice over 10 generations and thus C57BL/6 mice were used as a WT control. We newly generated Cav-1-floxed (Cav-1$^{flox/flox}$) mice, in which Cav-1 exon3 is flanked by two loxP sites on the C57BL6 background (UNITECH CO, Kashiwa, Japan). To generate eCav-1-KO mice, Cav-1$^{flox/flox}$ mice were cross-bred with Tie2-Cre mice (Jackson Laboratory, Bar Harbor, ME, USA).[2] The mice were subjected to ligation of the proximal left anterior descending coronary artery (LAD) to induce AMI.[3] They were randomly assigned to the 2 groups with (LIPUS group) or without (no-LIPUS group) the LIPUS therapy. In addition to the AMI groups, the sham-operated groups (with or without LIPUS therapy) were also made with the same procedure but without the LAD ligation. Animals were

excluded from the present study when LV fractional shortening (FS) exceeded 30 % at day 1. We stored the heart samples at 3, 6, 28, and 56 days after AMI. Animals were euthanized by cervical dislocation under anesthetic inhalation overdose with isoflurane. For mRNA and protein analysis, the heart was divided into infarcted (including adjacent border area) and remote area. For histological analysis, the heart was divided into infarcted, border and remote areas.

LIPUS Therapy

For the LIPUS therapy, we used a diagnostic ultrasound device (Prosound α10; HITACHI Aloka Medical, Ltd., Mitaka, Japan) whose irradiation conditions could be modified by software modification. Based on our previous studies,[4] we performed LIPUS therapy under the following conditions; frequency 1.875 MHz, pulse repetition frequency 4.90 kHz, number of cycles 32, voltage applied to each transducer element, 17.67-22.38 volts (V), and Ispta (spatial peak temporal average intensity) 117-174 mW/cm^2. The power of LIPUS was 0.25 W/cm^2, the beams were irradiated from the sector-shaped probe and were focused at 6 cm depth.[4] The number of cycles of pulsed ultrasound represents that of acoustic waves per 1 pulse, while 1 cycle is used for diagnostic ultrasound devices **(Supplemental Figure IA)**. The voltage applied to each transducer element was controlled to keep estimated Ispta of LIPUS below the upper limit of acoustic output standards (<720 mW/cm^2) for diagnostic ultrasound devices (US Food and Drug Administration's Track 3 Limits) and to prevent the ultrasound probe from temperature rise.[4] LIPUS was applied to mice or cultured cells through an agar phantom gel **(Supplemental Figure IB, IIIA)**. The attenuation coefficient of the phantom gel was almost comparable to that of living cells (muscles, fat, blood etc.). In in vivo studies, LIPUS was applied to the heart by 2-dimensional scan at 3 different short axis levels (aortic valve, mitral valve and papillary muscle levels for 20 min each) in a day

under inhalation anesthesia with 1.2% isoflurane.[4] The LIPUS group was subjected to the LIPUS therapy 3 times in the first week (1, 3 and 5 days after AMI), whereas the no-LIPUS group underwent the same procedures 3 times including anesthesia but without the LIPUS therapy **(Figure 1A)**.

Echocardiographic Evaluation

In order to follow up the time course of LV function after AMI, we performed transthoracic two-dimensional echocardiography (Vevo2100, Visual Sonics, Ontario, Canada) on mice anesthetized by inhalation of isoflurane (1-1.5%) before and at 1, 14, 28, 42 and 56 days after AMI **(Figure 1A)**.

Histopathological Analysis

Excised hearts were fixed with 4% paraformaldehyde for histological and immunohistochemical examination. After 24-48 hours of fixation and dehydration through increasing concentrations of ethanol, the tissue specimens were embedded in paraffin and sliced at 3μm in thickness. The sections were used for hematoxylin-eosin (HE, Sigma-Aldrich, Shinagawa, Japan), Masson-trichrome (MT, Sigma-Aldrich), immunohistochemical stainings for CD31 (anti-CD31, 1:400, Abcam, Cambridge, UK), immunodetection was accomplished using a Histofine kit (Nichirei, Tsukiji, Japan). The extent of infarct area was calculated as a rate of fibrotic area using the following formula: fibrotic area/(LV free wall + interventricular septum)×100 (%). Cross-sectional area of MT stained image was used to analyze the infarct area with the use of Image J Software (NIH). The number of immunopositive cells was counted in the infarcted, border and remote areas, where 6 random fields were examined in each sample at × 400 magnification in a blinded manner.

Real-time PCR in Vivo

We measured mRNA expression of vascular endothelial growth factor (VEGF), endothelial nitric oxide synthase (eNOS), and caveolin-1 in the LV. The heart samples were homogenized and used for mRNA extraction with an RNeasy Plus Universal kit (QIAGEN, Hilden, Germany). cDNA was synthesized by using PrimeScript RT Master Mix (Takara Bio Inc., Otsu, Japan). The primer sequences were as follows; VEGFA, (Forward) 5'-ACATTGGCTCACTTCCAGAAACAC-3' and (Reverse) 5'-TGGTTGGAACCGGCATCTTTA-3'; eNOS, (Forward) 5'-ATTCTGGCAAGACAGACTACACGA-3' and (Reverse) 5'-TCCCGGTAGAGATGGTCCAG-3'; caveolin-1, (Forward) 5'-TTTCACCTGTGTACCTGAGTCTCCA-3' and (Reverse) 5'-AAACAAGTCAAGCAGGGTTCCAA-3'; Klf2, (Forward) 5'-AGCTACACCAACTGCGGCAAG-3' and (Reverse) 5'-TCGCACAAGTGGCACTGAAAG-3'; GAPDH, (Forward) 5'-TGTGTCCGTCGTGGATCTGA-3' and (Reverse) 5'-TTGCTGTTGAAGTCGCAGGAG-3'.

After reverse transcription, real-time PCR was performed with SYBR Premix Ex Taq II (Takara Bio Inc) and CFX96^{TM} Real-Time system C1000^{TM} Thermal Cycler (Bio-Rad, Hercules CA, USA). The PCR conditions were 40 cycles of 2 sec at 98℃ and 5 sec at 55℃. mRNA expression levels were compared between the control and the LIPUS groups. Results are reported as the quotients of the copy number of the gene of interest relative to that of glyceraldehyde-3-phosphate dehydrogenase (GAPDH), as a housekeeping gene.

Western Blot Analysis in Vivo

A detailed list of antibodies used in the current study is supplied as supplemental material (**Supplemental Table I**). Protease and phosphatase inhibitor cocktails were from Sigma, St.

Louis, MO. Homogenized heart with the protease inhibitor cocktail and phosphatase inhibitor cocktail were centrifuged at 15,000 *g* for 15 min and protein concentration in the supernatant was determined with the bicinchoninic acid protein assay (#23225, Pierce, Rockford, IL). Equal amounts of proteins were subjected to SDS-PAGE and subsequently were electrotransferred to nitrocellulose membranes. The membranes were blocked for 1 hour at room temperature in 5% BSA in Tris-buffered saline with Tween 20 (TBS-T). Primary antibody incubations were performed at different dilutions as described in antibody list. All incubations for primary antibodies were done for overnight at 4℃. The secondary antibody was used at 1:4,000 dilutions for 1 hour at room temperature. Proteins were visualized by the enhanced chemiluminescence system (ECL Western Blotting Detection Kit, GE Healthcare) and quantified with the Image J Software (NIH). We measured protein levels of VEGF, eNOS, and phosphorylated ERK1/2 (pERK1/2) at Thr202 and Tyr204, total-ERK1/2 (tERK1/2), phosphorylated Akt (pAkt) at Ser473, total-Akt (tAkt), α-tubulin in the LV. The extents of expression of VEGF, eNOS, pERK1/2, pAkt were normalized by that of α-tubulin, tERK1/2, tAkt, respectively.

Effects of LIPUS on Human Endothelial Cells in Vitro

Human umbilical vein endothelial cells (HUVEC) from a single donor and human coronary artery endothelial cells (HCAEC) (Lonza, Basel, Switzerland) were cultured in a complete endothelial medium (EGM-2 BulletKit; Lonza). The cells were used at passages 3 to 5 and were maintained in EGM-2. Twenty-four hours before the LIPUS treatment, the cells (1×10^5) were re-suspended in a 2-ml tube with EGM (Lonza). They were exposed to LIPUS of 32 cycles (frequency, 1.875 MHz; pulse repetition frequency, 4.90 kHz; voltage, 22.38 volts (V); Ispta, 238 mW/cm^2) for 20 min (n=12 each). After irradiation, the cells were stored for 3, 6, 12 and 24 hours in the same medium before RNA extraction and for 0, 20 min, and 6, 12, 24, 36, 48 and 72 hours before protein extraction.

Scratch Assay

HUVECs were scratched with a pipette tip 24 hours after dissemination in the culture medium. After scratching HUVECs, the LIPUS was irradiated to the cells in the same manner as previously described. HUVECs were followed up for 48 hours after the irradiation. The length (pixel) of proliferation cells was counted.[5, 6]

Real-time PCR in Vitro

mRNA was extracted using the RNeasy Plus Mini kit (QIAGEN). mRNA (600ng) was reverse-transcribed using a QuantiTect Reverse Transcription kit (QIAGEN). Real-time PCR was performed using the Real-Time Detection System (Bio-Rad Laboratories). cDNA was synthesized by using PrimeScript RT Master Mix (Takara Bio Inc). The primer sequences were as follows;

VEGFA, (Forward) 5'-GAGCCTTGCCTTGCTGCTCTA-3' and (Reverse)
5'-CACCAGGGTCTCGATTGGATG-3'; eNOS, (Forward)
5'-AAAGACAAGGCAGCAGTGGAAAT-3' and (Reverse)
5'-TCCACGATGGTGACTTTGGCTA-3'; caveolin-1, (Forward)
5'-TTCTGGGCTTCATCTGGCAAC-3' and (Reverse)
5'-GCTCAGCCCTATTGGTCCACTTTA-3'; β1-integrin, (Forward)
5'-GGTTTCACTTTGCTGGAGATGG-3' and (Reverse)
5'-CAGTTTCTGGACAAGGTGAGCAATA-3'; Fyn, (Forward)
5'-CGGATTGGCCCGATTGATAG-3' and (Reverse)
5'-CACGTCAGACTTGATTGTGAACCTC-3'; FAK, (Forward)
5'-ACATTATTGGCCACTGTGGATGAG-3' and (Reverse)
5'-GGCCAGTTTCATCTTGTTGATGAG-3'; SDPR, (Forward)
5'-CTCCGACGCAACCATTTCA-3' and (Reverse) 5'-AAACACGCTGGCAGGGATCT-3';

GAPDH, (Forward) 5'-GCACCGTCAAGGCTGAGAAC-3' and (Reverse) 5'-TGGTGAAGACGCCAGTGGA-3', all of which were designed by the Perfect Real Time Support System (Takara Bio Inc).

Microarray Analysis in Vitro

To identify genes that are affected by LIPUS, we carried out Agilent SurePrint G3 Human GE 8×60K v2 Microarray analysis (Takara Bio Inc) of cells cultured 6 hours after LIPUS at 0.25 W/cm^2 for 20 min. Genes that were up- or down-regulated by >1.5-fold were examined using Agilent Feature Extraction software (Takara Bio Inc.). After the analysis of each HUVECs and HCAECs, we analyzed the pooled data of both cell types after revising with combat analysis to eliminate the batch effects lay between the two cell types. After the combat analysis, we performed the functional and pathway analysis of differentially expressed genes in the endothelial cells exposed to LIPUS using the Gene Ontology and KEGG Pathway database. Significant genetic networks were identified in the differentially expressed genes affected by LIPUS. The data are summarized in **Supplemental Table II.** Results were also analyzed through the use of QIAGEN's Ingenuity® Pathway Analysis (IPA®, QIAGEN Redwood City, www.qiagen.com/ingenuity).

Studies with siRNA

Pre-designed siRNA targeting human caveolin-1, β1-integrin, Fyn, focal adhesion kinase (FAK) and serum deprivation protein response (SDPR), and negative control siRNA were obtained from QIAGEN (caveolin-1 siRNA #S100299614, β1-integrin siRNA #S100300573, Fyn siRNA #S100605451, FAK siRNA #S100301532, SDPR siRNA #S103246789; QIAGEN, Tokyo, Japan). siRNA transfection was performed using HiPerFect Transfection Reagent (#301702; QIAGEN). Briefly, 0.5×10^6 cells were transfected in 2 ml of EGM-2 containing 500μl of HiPerFect Transfection Reagent and 100nM of siRNA.

Measurement of Phospho-protein by Bio-Plex System in Vitro

We also measured phosphorylated proteins using Bio-Plex Pro Human Phospho-protein custom plate and Bio-Plex 200 system according to the manufacturer's instructions (Bio-Rad Laboratories). We measured the phosphorylated proteins of the cultured cells harvested with Bio-Plex Pro Signaling Reagent kit (Bio-Rad Laboratories, #171-304006M) and phosphatase-treated HeLa (Bio-Rad Laboratories, #171-YZB001). We evaluated phosphorylated MEK1 at Ser217/Ser221, phosphorylated Erk1/2 at Thr202/Tyr204 and Thr185/Tyr187, phosphorylated p38 MAPK at Thr180/Tyr182, phosphorylated JNK at Thr183/Tyr185, phosphorylated c-Jun at Ser63, phosphorylated Akt at Ser473 and Thr308, phosphorylated p70 S6 kinase at Thr421/Ser424 and Thr389, phosphorylated NF-kB p65 at Ser536, phosphorylated IkB-a at Ser32/Ser36, phosphorylated EGFR at Tyr1173 and Tyr1068, phosphorylated VEGFR-2 at Tyr1175, phosphorylated PDGFR-a at Tyr754, phosphorylated PDGFR-b at Tyr751, phosphorylated IGF-1R at Tyr1131, phosphorylated HER-2 at Tyr1248, phosphorylated Smad2 at Ser465/Ser467, phosphorylated GSK-3a/b at Ser21/Ser9, phosphorylated Stat1 at Tyr701, phosphorylated Stat3 at Tyr705 and Ser727. Results were analyzed using the Bio-Plex Manager 4.1.1 software. All measurements were performed by Bio-Rad Research Solution Center with blinded manner.

Western Blot Analysis in Vitro

Cultured cells were harvested with cell lysis buffer (50mM Tris-HCl (pH 7.4), 150mM NaCl, 1mM EDTA, 0.25% sodium deoxycholate, 1% NP-40, with the protease inhibitor cocktail and phosphatase inhibitor cocktail. Cell lysates were centrifuged at 15,000 *g* for 15 min and protein concentration in the supernatant was determined with the bicinchoninic acid protein assay (#23225, Pierce). Equal amounts of proteins were subjected to SDS-PAGE and subsequently were electrotransferred to nitrocellulose membranes. The membranes were

blocked for 1 hour at room temperature in 5% BSA in Tris-buffered saline with Tween 20 (TBS-T). Primary antibody incubations were performed at different dilutions as described in antibody list. All incubations for primary antibodies were done for overnight at 4℃. The secondary antibody was used at 1:4,000 dilutions for 1 hour at room temperature. Proteins were visualized by the enhanced chemiluminescence system (ECL Western Blotting Detection Kit, GE Healthcare) and quantified with the Image J Software (NIH). We measured protein levels of VEGF, eNOS, and phosphorylated ERK1/2 (pERK1/2) at Thr202 and Tyr204, total-ERK1/2 (tERK1/2), phosphorylated Akt (pAkt) at Ser473, total-Akt (tAkt), phosphorylated Src (pSrc) at Tyr416, total-Fyn (tFyn), phosphorylated FAK (pFAK) at Tyr397, total-FAK (tFAK), α-tubulin. The protein levels of VEGF, eNOS and HUTS-4 were normalized to the levels of α-tubulin. The levels of pERK1/2, pAkt, pSrc and pFAK were normalized to those of tERK1/2, tAkt, tFyn, and tFAK.

Human Autopsy Samples

Human autopsy samples of coronary arteries were obtained from patients who died of AMI (N=15, 66±12 year-old, 11 males/4 females). Experimental samples were taken from the distal site of the culprit coronary artery, while samples from non-culprit coronary artery were also used as control samples. Immunohistochemical stainings for CD31 (#M0823; Dako, Tokyo, Japan), caveolin-1 (#3238; Cell Signaling, Danvers, USA) and β1-integrin (#4706; Cell Signaling) were performed. The expression of caveolin-1 was evaluated in a blinded manner by a semi-quantitative scoring system; no staining 0, weak staining 1, moderate staining 2, and strong staining 3.

Statistical Analysis

Continuous results are expressed as mean ± SD. We utilized Student's t-test followed by Bonferroni type multiple comparisons and 2-way ANOVA with Turkey's HSD multiple comparison test to compare mean values (GraphPad Prism Software Inc, San Diego, CA). Survival analysis was performed by the Kaplan-Meier method, and between-group differences in survival were tested by the log-rank (Mantel-Cox) test. For all tests, *P*-values < 0.05 were considered to be statistically significant.

Supplemental References

1. Ohashi J, Sawada A, Nakajima S, Noda K, Takaki A, Shimokawa H. Mechanisms for enhanced endothelium-derived hyperpolarizing factor-mediated responses in microvessels in mice. *Circ J*. 2012;76:1768-1779.
2. Kisanuki YY, Hammer RE, Miyazaki J, Williams SC, Richardson JA, Yanagisawa M. Tie2-cre transgenic mice: A new model for endothelial cell-lineage analysis in vivo. *Dev Biol*. 2001;230:230-242.
3. Aaron AM, Hermann JL, Weil BR, Wang Y, Tan J, Moberly SP, Fiege JW, Meldrum DR. Animal models of myocardial and vascular injury. *J Surg Res*. 2010;162:239-49.
4. Hanawa K, Ito K, Aizawa K, Shindo T, Nishimiya K, Hasebe Y, Tuburaya R, Hasegawa H, Yasuda S, Kanai H, Shimokawa H. Low-intensity pulsed ultrasound induces angiogenesis and ameliorates left ventricular dysfunction in a porcine model of chronic myocardial ischemia. *PLoS One*. 2014;9:e104863.
5. Shimizu T, Fukumoto Y, Tanaka S, Satoh K, Ikeda S, Shimokawa H. Crucial role of ROCK2 in vascular smooth muscle cells for hypoxia-induced pulmonary hypertension in mice. *Arterioscler Thromb Vasc Biol.* 2013;33:2780-91.
6. Liang CC, Park AY, Guan JL. In vitro scratch assay: a convenient and inexpensive method for analysis of cell migration in vitro. *Nat Protoc.* 2007;2:329-33.

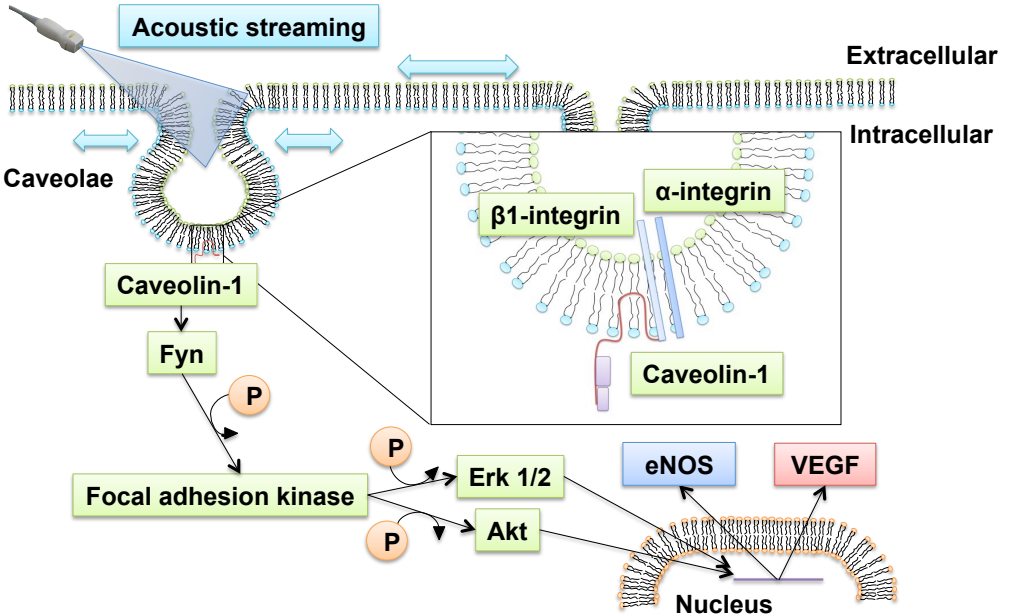
Acoustic streaming
Extracellular
Intracellular
Caveolae
β1-integrin
α-integrin
Caveolin-1
Caveolin-1
Fyn
P
P
Focal adhesion kinase
Erk 1/2
P
Akt
eNOS
VEGF
Nucleus